REPORT DOCUMENTATION PAGE

Form Approved
OMB No. 0704-0188

PLEASE DO NOT RETURN YOUR FORM TO THE ABOVE ORGANIZATION.

1. REPORT DATE *(DD-MM-YYYY)*	2. REPORT TYPE	3. DATES COVERED *(From - To)*
02-28-2012	Final Report	02/26/2009 - 11/30/2012

4. TITLE AND SUBTITLE
A Gas-Surface Interaction Model based on Accelerated Reactive Molecular Dynamics for Hypersonic conditions including Thermal Conduction

5a. CONTRACT NUMBER
FA9550-09-1-0157

5b. GRANT NUMBER

5c. PROGRAM ELEMENT NUMBER

6. AUTHOR(S)
Schwartzentruber, Thomas, E.
Tadmor, Ellad, B.
Cozmuta, Ioana

5d. PROJECT NUMBER

5e. TASK NUMBER

5f. WORK UNIT NUMBER

7. PERFORMING ORGANIZATION NAME(S) AND ADDRESS(ES)
Regents of the University of Minnesota
Office of Sponsored Projects Admin
200 Oak St. SE
Minneapolis, MN 55455

8. PERFORMING ORGANIZATION REPORT NUMBER

9. SPONSORING/MONITORING AGENCY NAME(S) AND ADDRESS(ES)
AF Office of Scientific Research
875 N Randolph St., Rm 3112
Arlington, VA 22203

10. SPONSOR/MONITOR'S ACRONYM(S)

11. SPONSOR/MONITOR'S REPORT NUMBER(S)
AFRL-OSR-VA-TR-2012-0982

12. DISTRIBUTION/AVAILABILITY STATEMENT
A - Approved for public release.

13. SUPPLEMENTARY NOTES

14. ABSTRACT
A finite-rate gas-surface interaction boundary condition was developed and implemented in a general unstructured 3D CFD solver. This boundary condition solves a user-defined set of gas-surface chemical reactions at each wall face in the computational grid, with corresponding reaction rates as input. The second focus was to use computational chemistry simulations to systematically determine the dominant catalytic reactions for oxygen-silica surfaces and also determine the activation energies and steric factors required to specify each reaction rate. The interatomic potential utilized was the ReaxFF potential designed specifically for silicon dioxide. Large-scale molecular dynamics (MD) simulations were used to simulate gas-surface chemical reactions. The techniques were then used to first characterize the catalytic defects on amorphous silicon-dioxide surfaces exposed to dissociated oxygen. The dominant reactions occurring on these defects were studied by MD simulations of oxygen impacts. Steric factors and activation energies were computed for each reaction and detailed balance was used to determine certain backwards rates. The result was a new finite-rate catalytic model predicted by computational chemistry simulations that can be directly used CFD calculations.

15. SUBJECT TERMS
High temperature gas-surface interactions
Molecular Dynamics
Computational Fluid Dynamics

16. SECURITY CLASSIFICATION OF:			17. LIMITATION OF ABSTRACT	18. NUMBER OF PAGES	19a. NAME OF RESPONSIBLE PERSON
a. REPORT	b. ABSTRACT	c. THIS PAGE			Thomas Schwartzentruber
UU	UU	UU	UU	29	19b. TELEPHONE NUMBER *(Include area code)* 612-625-6027

A Gas-Surface Interaction Model based on Accelerated Reactive Molecular Dynamics for Hypersonic Conditions including Thermal Conduction

Grant/Contract Number: FA9550-09-1-0157
Program Manager: Dr. John Schmisseur

PI: Thomas E. Schwartzentruber
Aerospace Engineering and Mechanics,
University of Minnesota
Phone: 612-625-6027 Fax: 612-626-1558 Email: schwartz@aem.umn.edu

Co-PIs: Ellad Tadmor (Aeropsace Engineering and Mechanics, University of Minnesota)
Ioana Cozmuta (ERC Inc., NASA Ames Research Center)

DOCUMENT CONTENTS:

I. Introduction and Existing State-of-the-Art

Vehicles traveling through an atmosphere at hypersonic speeds generate strong shock waves. These shock waves generate extremely high gas temperatures within the shock layer between the shock itself and the surface of the vehicle. As the gas reaches such high temperatures, its vibrational degrees of freedom become excited and diatomic and polyatomic molecules dissociate into reactive atomic species. At high altitudes characteristic of hypersonic flight where the free-stream density is low, these reactive species diffuse through the boundary layer and may chemically react with the vehicle's thermal protection system (TPS). Many TPS materials act as a catalyst for the heterogeneous recombination of dissociated species back into molecules. Such exothermic surface reactions transfer additional energy to the vehicle surface and thus contribute to the heat flux and overall heat load that the TPS must withstand. For example, studies have shown that surface catalysis can contribute up to 30% of the total heat load for Earth reentry [1].

Typically at the beginning of the design phase of a TPS, 100% catalytic efficiency is assumed at the vehicle surface. This provides an upper-limit, conservative estimation for the heating rates. For 100% catalytic efficiency, all dissociated atoms impacting the surface are assumed to leave the surface as recombined molecules. Later in the design cycle the boundary conditions may be relaxed to a parameterized catalytic efficiency (using a recombination rate γ, that is a function of temperature and pressure) if such data exists for the specific gas and solid conditions involved. As outlined in a recent review article on the status of aerothermal modeling [2], such data is very limited and contains large uncertainties. While lower and upper bounds on heating rates are certainly useful, depending on the flight conditions and atmosphere, these predictions can differ significantly. For example, the stagnation point heat flux for Mars entry varies by a factor of three between the assumptions of a highly- and weakly-catalytic wall [3]. An example of experimental data obtained on RCG coated Space Shuttle tiles [4] is shown below in Fig. 1. Here the atom recombination coefficient γ (for both oxygen and nitrogen atoms) is curve-fit to various functions of temperature.

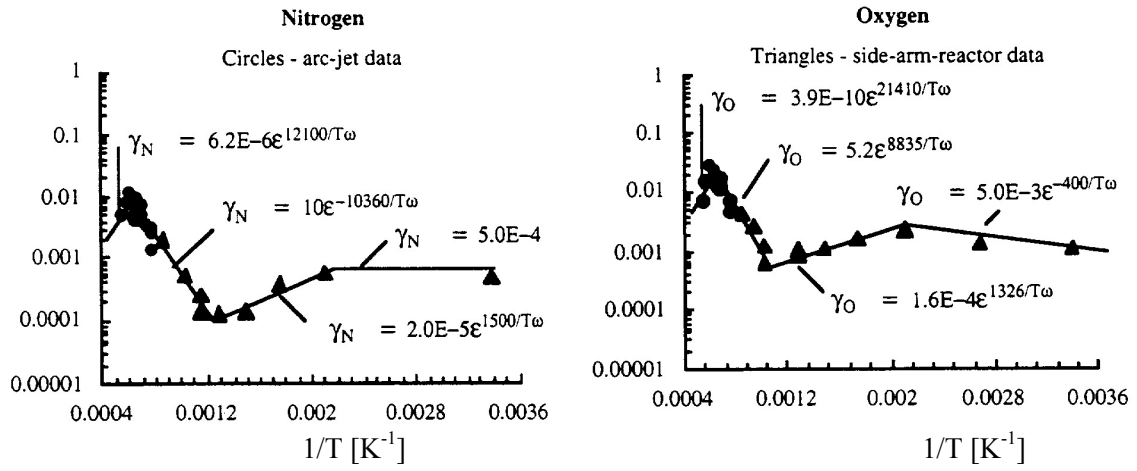

Figure 1 – Experimentally determined recombination rate (γ) as a function of temperature for RCG coated tiles (taken from [4] "Surface Catalysis and Characterization of Proposed Candidate TPS for Access-to-Space Vehicles", Stewart 1997).

Currently there is no fundamental explanation for these complex trends with temperature. It is possible the large changes in slope are due to different chemical mechanisms being "activated" at certain temperature thresholds, but these mechanisms are unknown. Inherently, the parameter γ represents the net effect of many elementary chemical mechanisms that collectively lead to recombination. As a result, it is difficult to relate variations in γ directly to fundamental surface chemistry. This inhibits a true

understanding of the phenomenon and limits the transferability of the model. Furthermore, the high temperature data, obtained in arc-jet tests, are inferred from heat flux measurements. This requires an accurate model of the arc-jet flow field and predicted convective heat flux. When compared with the measured heat flux, the discrepancy is attributed to recombination, where full energy accommodation is also assumed. In fact, the arc-jet flow is poorly characterized and the assumption of full energy accommodation is not necessarily valid. Thus, extrapolation of these inferred γ values to flight conditions is not rigorous.

II. Prior Research Efforts

II.1 Finite-Rate Gas-Surface Models

A more fundamental model for gas-surface chemistry is analogous to the gas-phase finite-rate chemistry models that have been successfully used for many years. However, **in practice, the *parameterization* of such finite-rate gas-surface interaction models is extremely challenging** [1,5-14]**.** For gas-surface systems, the chemical reactions now involve gas-phase species as well as adsorbed species, and reactions should be made specific to various "chemical sites" on the surface. As an example, a test model for air is listed in Table 1. The model contains air species N_2, O_2, N, O, NO, as well as adsorbed atomic species denoted as A(s), metastable (diffusing) adsorbed species $A(s)_m$, and finally open surface sites [s]. The reaction mechanisms include adsorption/desorption reactions as well as Eley-Rideal (E-R) and Langmuir-Hinshelwood (L-H) recombination reactions. E-R reactions occur when a gas-phase atom strikes an adsorbed atom and recombines into a molecule that leaves the surface. L-H reactions occur when two adsorbed atoms diffuse into close proximity and recombine to form a molecule that leaves the surface. Reverse reactions of these processes are also included.

$O + [s] \underset{k_b^1}{\overset{k_f^1}{\rightleftharpoons}} O(s)$		Adsorption/Desorption
$N + [s] \underset{k_b^2}{\overset{k_f^2}{\rightleftharpoons}} N(s)$		Adsorption/Desorption
$O + O(s) \underset{k_b^3}{\overset{k_f^3}{\rightleftharpoons}} O_2 + [s]$		E-R/Diss-Adsorption
$N + N(s) \underset{k_b^4}{\overset{k_f^4}{\rightleftharpoons}} N_2 + [s]$		E-R/Diss-Adsorption
$O + N(s) \underset{k_b^5}{\overset{k_f^5}{\rightleftharpoons}} NO + [s]$		E-R/Diss-Adsorption
$N + O(s) \underset{k_b^6}{\overset{k_f^6}{\rightleftharpoons}} NO + [s]$		E-R/Diss-Adsorption
$O(s)_m + O(s) \underset{k_b^7}{\overset{k_f^7}{\rightleftharpoons}} O_2 + 2[s]$		L-H/Diss-Adsorption
$N(s)_m + N(s) \underset{k_b^8}{\overset{k_f^8}{\rightleftharpoons}} N_2 + 2[s]$		L-H/Diss-Adsorption
$O(s)_m + N(s) \underset{k_b^9}{\overset{k_f^9}{\rightleftharpoons}} NO + 2[s]$		L-H/Diss-Adsorption
$N(s)_m + O(s) \underset{k_b^{10}}{\overset{k_f^{10}}{\rightleftharpoons}} NO + 2[s]$		L-H/Diss-Adsorption

Table 1 – Gas-surface reactions for a generic air surface catalysis model.

The net flux mediated by the surface depends on the dynamics of each species on the active surface sites according to the mechanisms listed and on the rate constants associated with each mechanism. For example, the specific form of the E-R rate constant is shown in Table 2 with an initial qualitative parameterization [5]. Currently there is no way of experimentally determining all the required parameters and rate coefficients. However, these **parameters now have a direct physical link to fundamental chemistry**. Specifically, the coefficients correspond to activation energies (E), steric factors (γ), surface site concentrations (Φ_{total}), and kinetic flux quantities ($v/4$). In principle, the reaction mechanisms and parameters required for their rates could be

$$Eley - Rideal$$
$$\gamma_{er,O} = 0.001$$
$$\beta_O = 0$$
$$E_{er} = 9000\ J/mol$$
$$\Phi_{total} = 7.5 \times 10^{-6}\ mol/m^2$$

$$k_f = \left(\frac{\bar{v}}{4\Phi_{total}}\right)\gamma_o T^{\beta} \exp\left(-\frac{E_{er}}{RT}\right)$$

Table 2 – Example of a test parameterization for the forward reaction rates.

determined by computational chemistry studies. Indeed, this approach has been successful for many *gas-phase* finite-rate chemistry models currently in use and our research attempts to accomplish this for gas-surface finite-rate chemistry.

II.2 Computational Chemistry Studies of *Unphysical* Crystalline Surfaces

A substantial amount of previous research had been conducted in this area by two European research groups; one located in Bari, Italy [15-16] and the other in Barcelona, Spain [17-21]. In fact, the group from Spain recently published an article (in 2011) where a finite-rate catalytic model is developed for air-silica interactions using computational chemistry simulations [21]. We have performed a thorough review of this prior work since it is so closely related to the main objectives of this AFOSR grant. Unfortunately, **during the early stages of our research for this grant, we quickly realized that these prior methodologies were completely inadequate for real materials used in hypersonic applications, and we found the conclusions of many of these studies to be invalid.** Since this AFOSR research report will present a new oxygen-silica finite rate catalytic model that is substantially different from this previously published work, a critical review of this prior work is warranted. A brief review follows that clearly **shows a large disconnect between the computational chemistry community and the aerothermodynamics community** for these problems and highlights some of the critical issues addressed by our AFOSR grant research.

Unphysical Bulk Material (Prior Studies):

Both research groups used computational chemistry techniques to investigate oxygen interactions with a specific crystalline polymorph of SiO_2 (called β-cristobalite). Computer images of this crystal lattice are shown in Fig. 2. The choice of β-cristobalite is motivated by experimental studies from Balat-Pichelin *et al.* [15,22,23] where silicon-carbide (SiC) surfaces were exposed to high temperature air-plasmas. During such exposure, an oxide layer was quickly formed and atomic oxygen loss-rates (recombination coefficients) were then determined next to the oxide layer surface. While the experimental measurements are of high quality and repeatability, the conclusion that the measured loss rates correspond to β-cristobalite was based on the fact that for polymorph diagrams of SiO2, β-cristobalite is most stable within the experimental surface temperature range. However, **it is almost impossible to imagine that a crystalline oxide layer was formed by exposing SiC to an air plasma**. Indeed, production of crystalline materials (such as quartz, another stable SiO_2 polymorph) requires careful and precise manufacturing techniques to slowly grow the crystal without introducing defects. Thus, **these prior studies are computationally investigating a different material than used in the experiments they compare with.** Rather, the oxide layer produced in the experiments is most likely amorphous SiO_2.

Unphysical Surface Structure (Prior Studies):

Furthermore, in order to simulate interactions with a *surface*, these prior studies simply "cleaved" the bulk crystal along the (001) plane (as seen in Fig. 2a) and then proceeded to study gas-phase collisions with this surface. However, such cleaved surfaces have highly unphysical dangling bonds (see the top layer of Si atoms in Fig. 2a). For example, these studies conclude (and we have confirmed) that any gas-phase oxygen that hits these dangling bonds will immediately adsorb (as seen in Fig 2b) with such a strong bonding energy that no future catalytic reaction could possibly remove this atom from the surface to form a molecule.

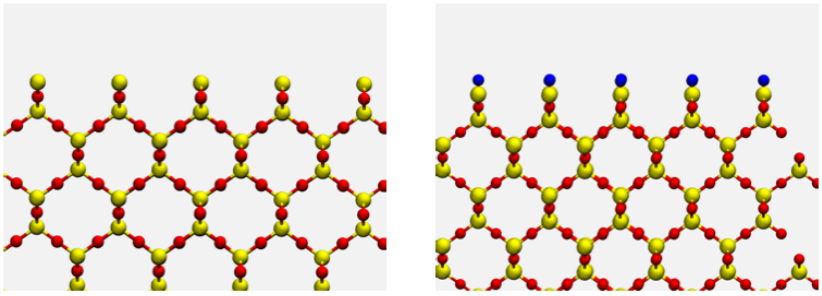

(a) Silicon Terminated (001) β-Cristobalite Surface (side)

(b) Oxygen Terminated (001) β-Cristobalite Surface (side). Topmost layer of oxygen highlighted in blue.

Figure 2 – Cleaved (001) β-cristobalite surfaces used in prior computational chemistry studies of surface catalysis under conditions relevant to hypersonic flight (Si – yellow, O – red, O originating from the gas are blue).

In order to study recombination, these previous studies instead placed adsorbed oxygen atoms at different (and less energetically bound) locations and then studied collisions with incoming gas-phase oxygen atoms. This now led to a certain rate of recombination reactions, which of course depended upon where the adsorbed oxygen was placed. By following this invalid modeling approach, remarkable agreement with measurements from air plasma experiments was reported [15,16]. In contrast, our computational chemistry simulations predict that such cleaved surfaces reconstruct into the lower-energy, stable surface configurations seen in Fig. 3. Such surface reconstructions are supported by a number of experimental studies that will be detailed later in this report. Thus, **not only is the bulk material (β-cristobalite) unphysical but, perhaps more importantly, the *surfaces* that gas-phase atoms interact with in these previous studies are not only physically unrealistic, but they are computationally unstable.**

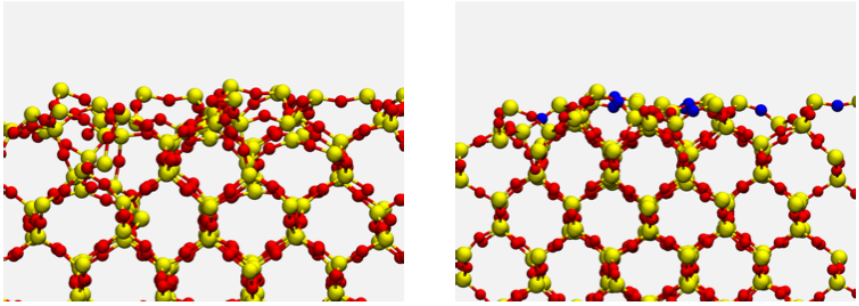

(a) Silicon Terminated (001) β-Cristobalite Surface (side)

(b) Oxygen Terminated (001) β-Cristobalite Surface (side). Topmost layer of oxygen are highlighted in blue.

Figure 3 – Surface reconstructions of (001) β-cristobalite (Si – yellow, O – red, O originating from the gas are blue).

Arbitrary Surface Coverage (Prior Studies):

Once probabilities of adsorption, desorption, and recombination are determined in function of surface temperature and gas-phase impact energy, one can develop a reaction rate model parameterized in function of the gas-surface temperature (T). If these rate equations are solved for a given partially-dissociated gas state (species concentrations, temperature, and pressure), the resulting concentrations of adsorbed species [A(s)] can be calculated from the reactions in Table 1. These adsorbed concentrations then correspond to a specific surface coverage corresponding to these specific gas conditions. **Determination of the surface coverage is extremely important, as it dictates the actual surface that gas-phase molecules interact with**. In the previously published finite rate model [21], the model predicted a steady-state coverage saturated with O_2 molecules for which no further recombination is

possible. However, a surface coverage part-way between zero coverage and steady state was selected and recombination efficiencies for this arbitrary coverage were reported, which also happened to match experimentally determined values very well. There is no basis for assuming such an arbitrary surface coverage. In fact, a steady state surface coverage is established over very small time scales while catalytic reactions continue on the surface for macroscopic time scales. Thus, **the surface coverage assumed in prior studies was not representative of the experiments they compared with, and was even in contradiction with the computational chemistry simulations of the same studies.**

Improper Application of Detailed Balance and Unphysical Backwards Rates (Prior Studies):

Finally, as will be shown from our research, when forming a finite-rate chemistry model, **detailed balance must properly be accounted for such that reverse reaction rates and equilibrium states remain physically realistic**. Specifically, in the previously published rate model [21], the reverse rate of E-R recombination (dissociative adsorption of a gas-phase molecule) is very high and roughly equal to that of atomic oxygen adsorption. However, the O_2 surface impact simulations presented in the same publication do not find any dissociative adsorption reactions despite finding an atomic adsorption probability close to one. Furthermore, the reported desorption rate coefficient is higher than the theoretical limit (set by the vibrational frequency of O_2 molecules) by two orders of magnitude. Thus, this **previously published finite-rate catalytic model for oxygen-silica interactions contains backwards rates that are both unphysical and in contradiction with the computational chemistry simulations themselves.**

These prior studies [15-21] have been published in high quality computational chemistry and surface science journals. The above critical review clearly demonstrates the lack of rigorous collaboration and understanding between computational chemistry researchers and aerothermodynamics researchers. Specifically, the conclusions of our research under this AFOSR grant are that each of the above aspects, bulk material, surface structure, surface coverage, and detailed balance are crucial to developing a physically realistic and consistent finite rate model for oxygen-silica catalytic reactions.

II.3 Computational Chemistry Studies of Amorphous SiO_2 Surfaces

Co-PI, Dr. Cozmuta, published an AIAA conference paper in 2007 entitled, "Molecular mechanisms of gas surface interactions in hypersonic flow" [24]. In this paper, Cozmuta presented preliminary results for computational chemistry simulations of dissociated air interacting with an *amorphous* SiO_2 surface. The simulations began with a vacant amorphous SiO_2 surface exposed to partially-dissociated high temperature air. Recombination reactions were monitored only after the surface coverage reached a steady state. An image of such a simulation is shown in Fig. 4. This type of simulation is much more physically realistic than those performed in the studies reviewed above, and **co-PI Cozmuta's work provided the original framework for our AFOSR grant research**. Specifically, Cozmuta chose to use a reactive force-field to model inter-atomic forces, called ReaxFF. The unique ReaxFF formulation enables large scale Molecular Dynamics (MD) simulation while accurately modeling chemical reactions. ReaxFF will be described in detail in an upcoming section of this report.

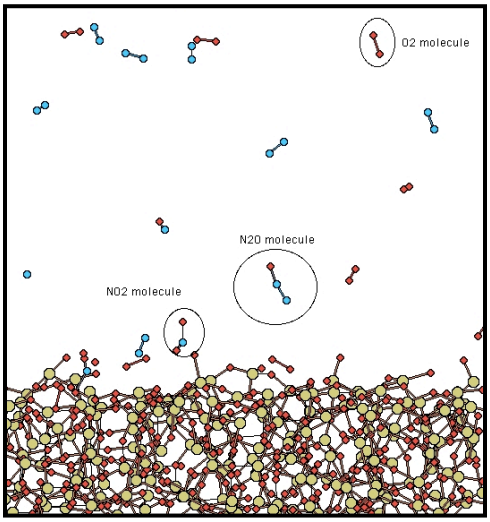

Figure 4 – ReaxFF MD simulations of dissociated air interacting with amorphous SiO_2.

III. AFOSR-Grant Research Accomplishments

Overview of main accomplishments

The accomplishments are subdivided into the following four main subsections:

III.1 Implementation of a Finite-Rate-Catalytic Boundary Condition in the US3D CFD Code

- a new finite-rate catalytic (FRC) wall boundary condition has been implemented in the US3D CFD developed and maintained at the University of Minnesota
- this FRC boundary condition solves a set of user-specified chemical reactions at all wall elements in a general 3D unstructured CFD simulation
- the implementation has been extensively validated with an independent implementation of the same technique in the NASA DPLR code through code-to-code comparisons
- the behavior of this type of boundary condition was investigated by using various test models and a number of useful conclusions drawn through Monte Carlo uncertainty analysis

III.2 Computational Chemistry: Inter-atomic Potential and Validation for Oxygen-Platinum Systems

- since the most well-studied surface catalysis problem in science is the oxygen-platinum system, the Molecular Dynamics potential (ReaxFF) and simulation techniques were validated extensively with existing experimental and literature data
- specifically, new simulation methods were developed using ReaxFF to predict surface coverage of oxygen on platinum, as well as model collisions of gas-phase oxygen with platinum (sticking and scattering angles), and validated with high quality experimental data

III.3 Quasi-Continuum Method: Heat Transfer from Surfaces into the Bulk Material

- here the QC method is extended to include heat transfer
- unsteady heat pulses are examined through atomistic systems

III.4 Computational Chemistry: A New Finite-Rate Catalytic Model for Oxygen-Silica

- here a finite-rate catalytic model (FRC) is developed from ReaxFF MD simulations for oxygen-silica systems

In contrast to any prior work, all of the following physical considerations are accounted for:

- amorphous bulk silica and resulting amorphous surface structure
- surface defects inherent in the amorphous silica structure
- defect structures and surface coverage resulting from exposure to high temperature oxygen
- catalytic reaction mechanisms specific to these defect chemistries
- determination of activation energies and steric factors for each catalytic reaction
- accounting for the effects due to off-normal collisions on reaction rates
- formulation of a complete finite-rate model ensuring detailed balance for backwards rates
- validation of the finite-rate model with existing experimental data

The result is a new finite rate model for air-silica gas-surface interactions that can be used directly with the new CFD FRC boundary condition developed in III.1 above.

III.1 Implementation of a Finite-Rate-Catalytic Boundary Condition in the US3D CFD Code

A finite-rate catalytic (FRC) wall boundary condition has been implemented and validated in the US3D CFD code developed and maintained at the University of Minnesota [25]. The user is able to specify a general set of gas-surface chemical reactions (such as those listed in Table 1), as well as the parameters required for the rates of each reaction (such as those in Table 2). The implementation chosen for this boundary condition is straightforward but effective. The chemical rate equations are solved in a separate subroutine and the result is used to simply re-set the species mass fractions in all 'ghost-cells' in a standard 3D unstructured CFD solver at each time step. Thus, **no modifications to the core CFD solver itself are required, and we believe this technique could be adopted easily by other research groups**. We then investigated the general behavior of this type of boundary condition by using a test parameterization for air-silica interactions from Marschall et al. [5], resulting in a number of important conclusions.

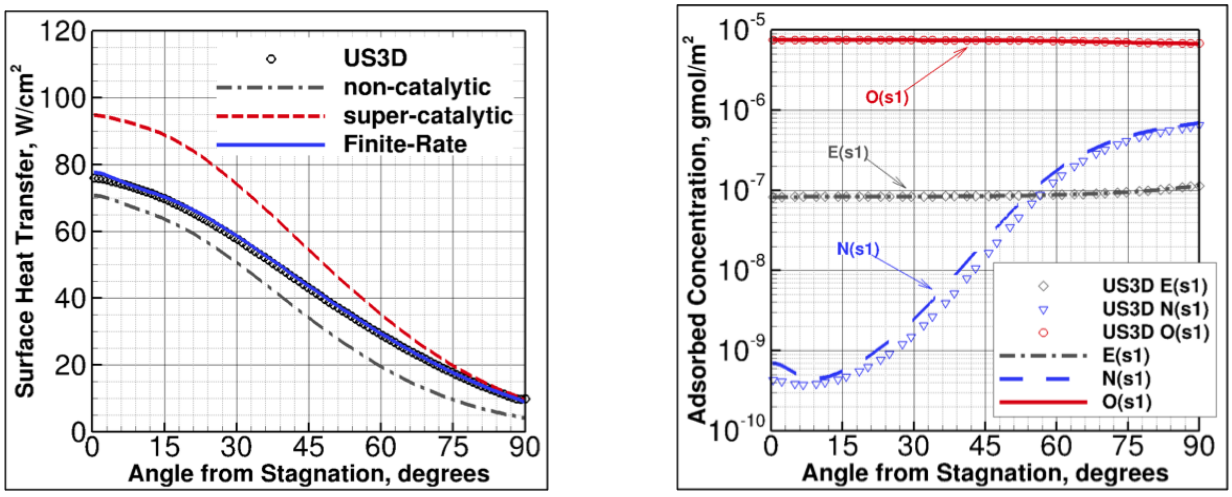

(a) (b)

Figure 5 – Comparison of US3D and DPLR results for surface heat flux (a) and for surface coverage (b).

Example results from US3D + FRC boundary condition are shown in Fig. 5 along with results from NASA's DPLR code. Specifically, heat flux results for 6 km/s air-flow over a 2m diameter cylinder (T=200K, ρ=0.001kg/m^3, T_{wall}=2250K), using the oxygen-silica model from Table 1 [5] are shown in Fig. 5a. The new FRC wall boundary condition predicts a heat flux between the limiting assumptions of super-catalytic and non-catalytic as expected. The corresponding surface coverages (O(s), N(s), and empty sites [s]) around the cylinder are shown in Fig. 5b. More importantly, the **US3D results have been compared with an independent finite-rate model implemented in the NASA DPLR code**. Both simulations employ the same gas-phase and gas-surface chemical reactions and rates, and **despite substantially different numerical implementations, the agreement is excellent**. These results were presented in a series of papers at the AIAA Thermophysics Conference in June 2011 [5,14,26].

A number of new contributions and conclusions resulted from this research, including:

1) Zero-dimensional gas-surface simulations were used to demonstrate that the **backwards rates of surface recombination reactions cannot be specified arbitrarily**. Rather, if the forward surface recombination rate is specified, the backwards rate is uniquely determined by the adsorption/desorption equilibrium constant as well as the gas-phase dissociation equilibrium constant. If rates are not prescribed in this manner, the system is shown to drift from its equilibrium state, a situation that, physically, should not be caused by a catalyst.

2) It was found that under certain conditions, despite a constant surface temperature, the recombination efficiency for oxygen atoms (γ_O) increased by a factor of 4 between the stagnation and 90 degree points

on the cylinder. This result can be seen in Fig. 6a and demonstrates how **recombination coefficients may not only be dependent on surface temperature, but also on surface coverage** which is a non-liner result of local gas-phase concentrations and numerous interacting gas-surface mechanisms. This is in contrast to existing models (such as shown previously in Fig. 1) that model γ as a function of temperature only.

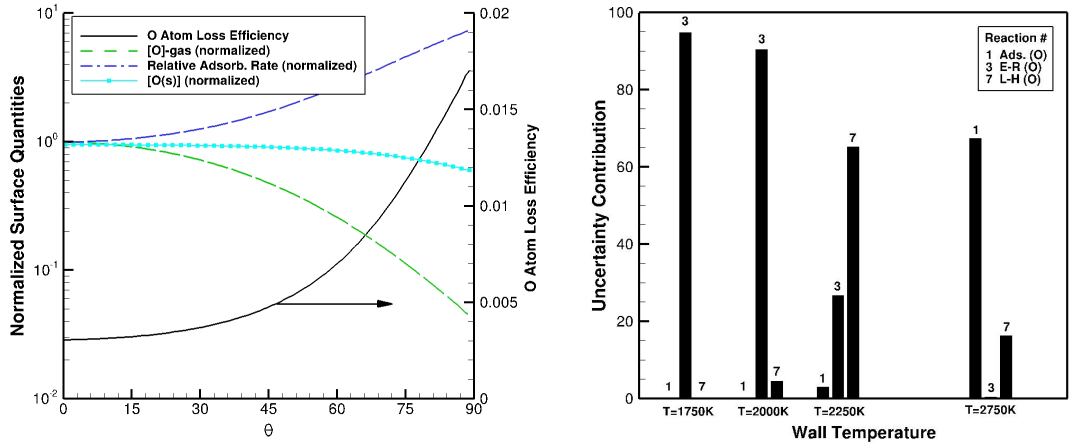

(a) (b)

Figure 6 – Variation of γ due to surface coverage on a constant temperature cylinder (a). Dominant reaction mechanisms contributing to stagnation point heat flux determined from Monte Carlo uncertainty analysis (b).

3) A finite-rate catalytic model introduces a large number of parameters that require specification, many of which are currently have large uncertainty. Thus **a legitimate concern involves uncertainty quantification for such a finite rate model as a whole.** To address this, Monte Carlo uncertainty analysis was performed (involving >1000 individual CFD solutions), where each rate was drawn from a log-normal distribution with roughly an order-of-magnitude variation. Correlation of stagnation point heat flux to each gas-surface reaction rate was performed. Uncertainty in the stagnation point chemical heat flux (q_c) was found to be directly linked to uncertainty in the dominant reaction rate at the surface temperature considered. The progression of dominant reactions as wall temperature is increased is shown in Fig. 6b, where the reaction numbers match those in Table 1. It is our conclusion that **careful analysis of a specific gas-surface interaction will often enable model reduction to a few dominant reactions where uncertainty can be well quantified.**

4) Finally, at a given surface temperature, our Monte Carlo analysis showed that an increase in the chemical heat flux (due to a variation in the reaction rates) leads to a fraction of that increase in the total heat flux. This implies that **although an increase in surface reactivity increases the chemical heat flux, it alters the boundary layer in a manner that decreases the conductive heat flux.**

III.2 Computational Chemistry: Inter-atomic Potential and Validation for Oxygen-Platinum Systems

The ReaxFF Interatomic Potential Model for Molecular Dynamics (MD) Simulations

For our computational chemistry simulations we use the ReaxFF potential. This potential is reactive in nature and provides an accurate description of dissociation and reaction curves [27,28]. The system energy in ReaxFF is divided into partial energy contributions similar to those of empirical nonreactive force fields (bond angle, torsion, van der Waals, and Coulomb) with the distinction that, in ReaxFF, all these contributions are bond order dependant and the nonbinded interactions (van der Waals and Coulomb) are included for all atom pairs to ensure continuity in the energy description during bond dissociation:

$$E_{system} = E_{val,bond} + E_{val,angle} + E_{val,torsion} + E_{vdWaals} + E_{Coulomb} + E_{lp} + E_{over} + E_{under} + E_{pen} + E_{conj}$$

The bond order dependence allows a smooth transition from nonbonded to single, double, and triple-bonded systems by ensuring that the corresponding energetic contributions disappear upon bond dissociation. In general ReaxFF is trained to an extensive database of DFT energies, however, it enables the simulation of large atomic systems (>1 million atoms if necessary). **Since the interatomic potential is the fundamental model used in our Molecular Dynamics (MD) simulations, the ReaxFF formulation and specific parameterizations for materials of interest must be validated with theory and experiment to the greatest extent possible.** Due to the automotive industry, **a large amount of experimental data and prior research focuses on oxygen-platinum catalytic systems**. Since platinum is also used in thermocouples used to measure heat flux in high enthalpy facilities, we first validated our numerical methods for oxygen-platinum systems.

Molecular Beam Experiments for Oxygen Impacting Pt(111)

The molecular dynamics technique with the ab initio based classical reactive force field ReaxFF was used to study the adsorption dynamics of O_2 on Pt(111) for both normal and oblique impacts. Overall, good quantitative agreement with the experimental data was found at low incident energies. Specifically, ours were the first numerical simulations to reproduce the characteristic minimum of the trapping probability at kinetic incident energies around 0.1 eV. This feature is well documented experimentally and our modeling revealed this minimum is due to the presence of a physisorption well near the surface, combined with the progressive suppression of a steering mechanism when increasing the translational kinetic energy or the molecule's rotational energy because of steric hindrance. In the energy range between 0.1 and 0.4 eV, the sticking probability increases, similar to molecular beam sticking data. For very energetic impacts above 0.4 eV, ReaxFF predicted sticking probabilities lower than experimental sticking data by almost a factor of 3 due to an overall less attractive ReaxFF potential energy surface compared to experiments and density functional theory.

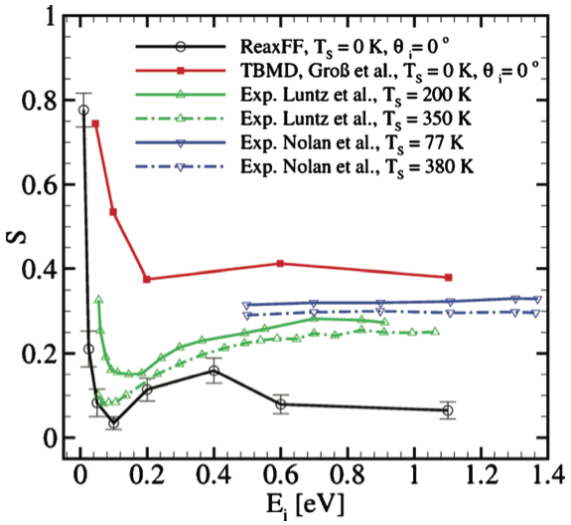

Figure 7 – Sticking probability for O_2 collisions with Pt(111) in function of impact energy. ReaxFF result is in black.

For oblique impacts, the trapping probability was reduced by the nonzero parallel momentum because of the PES corrugation and does not scale with the total incident kinetic energy. Furthermore, our simulations predicted quasispecular and slightly supraspecular distributions of angles of reflection, in accordance with molecular beam experiments. Increasing the beam energy to 1.7 eV caused the angular

distributions to broaden and to exhibit a tail toward the surface normal because molecules have enough momentum to get very near the surface and thus probe more corrugated repulsive regions of the PES.

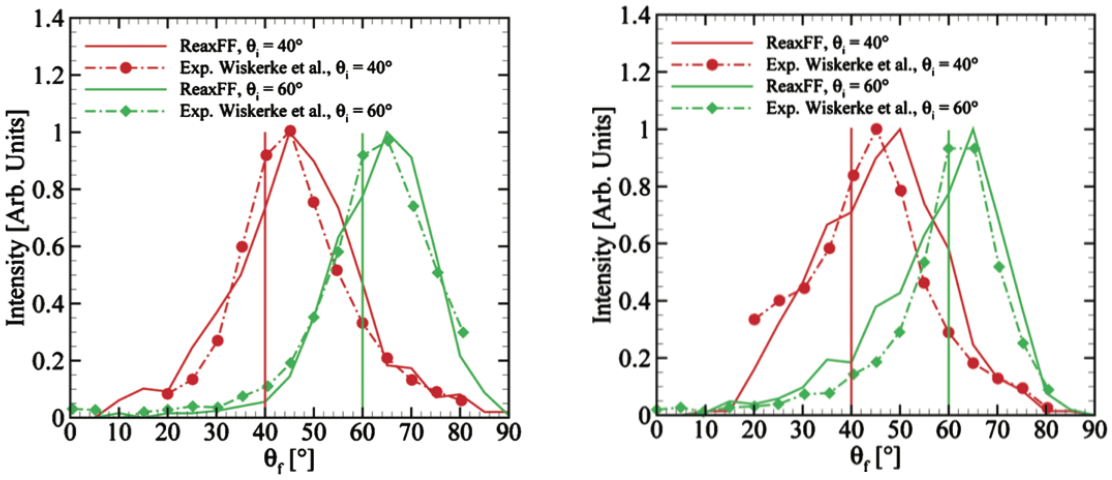

(a) (b)

Figure 8 – Scattering angles for O_2 collisions with Pt(111) at incident angles of 40° (red) and 60° (green). ReaxFF predictions compared to experimental measurements for two incident energies: 0.46 eV (a) and 1.73 eV (b).

Dissociative Adsorption of Oxygen on Pt(111) and Surface Coverage

In order to investigate gas-phase collisions with a material surface, **one must characterize the state of the surface (the surface coverage) that exists under the desired experimental or flight conditions**. Since **it is *this* surface that gas-phase molecules actually interact with** under conditions of interest. We developed a new technique that combines the ReaxFF potential with a statistical Monte Carlo technique to predict the oxygen coverage on a platinum surface in function of gas temperature and pressure and compared the predictions with extensive experimental results.

The most suitable ensemble to study adsorption problems is the so-called grand canonical ensemble (usually denoted with μ, V, T), where the temperature (T), volume (V), and chemical potential (μ) are fixed [29,30]. The gas is assumed to be in thermal equilibrium with the surface, i.e., $T = T_S$. At equilibrium, the chemical potential of a gas X adsorbed on a surface M and the chemical potential of X in the reservoir are equal, specifically:

$$\mu_{M\text{-}X} = \mu_X$$

The Grand Canonical Monte Carlo (GCMC) method is therefore an equilibrium technique to sample observables in the μ,V,T ensemble, for example the average number of particles adsorbed on the surface (or equivalently the surface coverage θ) at a prescribed chemical potential μ.

The standard GCMC algorithm [29] proceeds through two steps:

(1) Displacement of a particle: a random particle at x is selected and given a random displacement δx. This move is accepted with probability:

$$\mathbf{ACC(x \rightarrow x + \delta x) = \min(1, \exp\{-\beta[U(x + \delta x) - U(x)]\})}$$

(2) Insertion or removal of a particle: a new particle is inserted at a random position in the volume V or a random particle in V is removed. The insertion is accepted with probability:

$$\mathbf{ACC(N \rightarrow N+1) = \min(1, V/(\Lambda^3(N + 1)) * \exp\{\beta[\mu - U(N+1) + U(N)]\})} \ ,$$

and the removal is accepted with probability

$$\mathbf{ACC(N \rightarrow N-1) = \min(1, \Lambda^3 N/V * \exp\{-\beta[\mu + U(N-1) - U(N)]\})} \ .$$

Here, $\beta = 1/k_B T$ (k_B is Boltzmann's constant) and $\Lambda = [h^2/(2\pi m k_B T)]^{0.5}$ is the thermal de Broglie wavelength (h is Planck's constant and m is the particle mass). The potential energy of the system U is obtained from the ReaxFF potential and calculated by the Lammps MD package [31,32] (distributed by Sandia National Lab), which can be compiled as a set of external routines called by a driver program. The use of Lammps allows the simulation of fairly massive systems, because the calculation of the potential energy is done in parallel.

For an ideal diatomic gas X_2, the chemical potential is written as:

$$\mathbf{\mu = \mu^0_{X2}(T,p^0) + k_B T \ln(p_{X2}/p^0)}$$

where $\mu^0_{X2}(T,p^0)$ is a reference chemical potential that is only a function of T, and p_{X2} is the pressure in the reservoir. $\mu^0_{X2}(T,p^0)$ is either tabulated or can be calculated with the partition function of the gas (a known quantity).

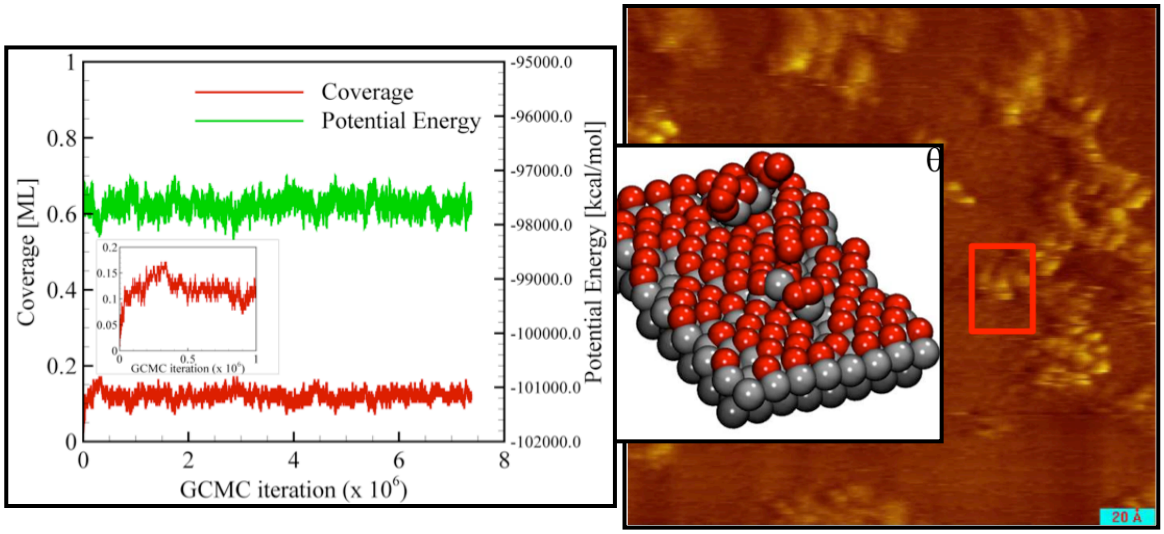

Figure 9 – GCMC convergence of surface coverage (left). GCMC prediction of high oxygen coverage and displaced Pt atoms displayed with experimental image (right).

Thus, specifying the chemical potential is equivalent to specifying the T, p conditions of the gas next to the surface. We performed such GCMC simulations for the well-studied problem of oxygen adsorbing on platinum (111), for which substantial theoretical, numerical, and experimental data exists. The results were very promising, some of which are shown in Fig. 9. Specifically, starting from a vacant Pt(111) surface, using the GCMC technique, equilibrium surface coverages were obtained for a wide variety of T, p conditions (even for p approaching near vacuum conditions). At these low pressures, the GCMC method predicted the well-known 0.25 mono-layer (ML) coverage and also predicted the specific p2x2 arrangement of adsorbed oxygen atoms in agreement with accepted experimental evidence. The method was also able to predict high surface coverages where Pt atoms are actually displaced out of the lattice, in qualitative agreement with experimental images (seen in Fig. 9).

These simulations are novel since they rely solely on a reactive interatomic potential (ReaxFF) to predict the chemical structure of the surface without pre-specification of expected surface structures common to other methods. In addition, the technique is highly consistent in that the same interatomic potential can be used for dynamic MD simulations. Therefore **enabling the prediction of the *in-situ* surface structure at low pressures and high temperatures, followed by the simulation of gas molecules interacting with this surface.**

III.3 Quasi-Continuum Method: Heat Transfer from Surfaces into the Bulk Material

In our Molecular Dynamics simulations of gas-surface interactions we thermostat our atomic surface system to a certain temperature T, and assume that this is representative of an experiment where the surface temperature is reported as the same T. However, the question arises, is the temperature of the first few atomic layers (important for catalytic reactions) actually the same as the temperature of the bulk material? More specifically, how is heat (perhaps deposited due to a catalytic reaction) transferred from these atomic surface layers into the bulk? Secondly, if we can study heat transfer at the atomic level as phonons transporting energy within the solid material, then it may be possible to determine correlations between the phonon properties of a material and the vibrational state of molecules leaving the surface. This would enable a much more physical understanding of the energy accommodation coefficient (β) that is typically assumed to be one for hypersonic flows. These questions motivated fundamental research into heat transfer processes spanning atomistic to continuum scales. The Quasi Continuum (QC) method of co-PI Tadmor was chosen as the methodology for this research. The QC method rigorously couples atomistic simulation to Finite Element continuum simulation for multi-scale material problems.

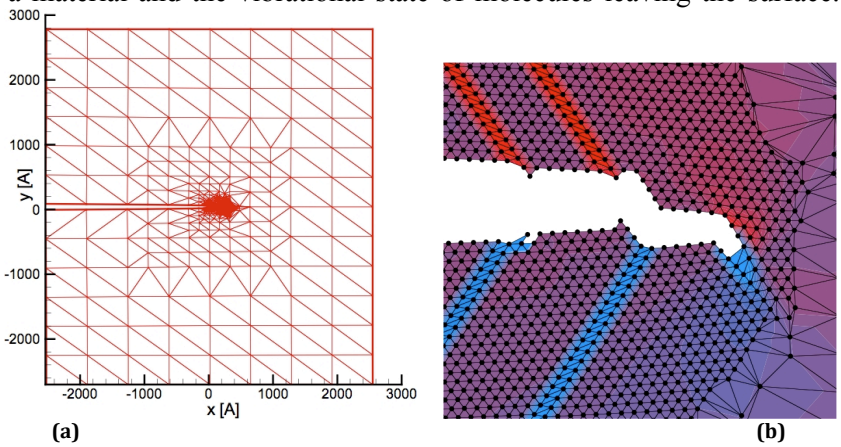

QC simulation of crack propagation in nickel. (a) The full model. The mesh has adapted to allow the crack to grow. (b) Detail of the crack tip. The colors correspond to contours of shear strain left in the wake of dislocations that have been emitted from the crack tip during its motion.

The QC method has been applied to a range of problems in atomic-scale mechanics, such as fracture and plasticity at the nanoscale. An example of a QC simulation of crack propagation is shown above (image right). Frame (a) shows the full QC model corresponding to a domain of 0.5mm×0.5mm, most of which is treated by the continuum limit of the method. Frame (b) shows a close-up of the tip of the propagating crack, which is described with full atomistic detail. This example shows the capability of QC to correctly capture the far-field continuum behavior while still being able to describe the atomistic processes of bond breaking and dislocation nucleation occurring at the crack tip.

The QC formulation prior to this grant was a zero-temperature minimization scheme. Formulation of a finite-temperature, "hot"-QC method has proven to be a very challenging proposition. The key difficulty is how to account correctly for the entropy of the atoms that have been integrated out of the continuum region. Clearly a coarse-grained node vibrating in the continuum region is not the same thing as an atom vibrating in the atomistic region. Consequently, the naive methodology of simply "doing dynamic" by solving Newton's equation for the full system (adopted in some multiscale methods) cannot be correct. Our objective was to use hot-QC to explore the effect of heat transfer between the atomistic region at the surface of the solid and the bulk continuum. This means that hot-QC must be extended from a constant temperature equilibrium method, to one in which a non-uniform temperature field can exist.

In this sense understanding heat diffusion in the material becomes important and the question whether non-stationary heat conduction is adequately modeled by Fourier's model or whether non-Fourier models, such as the Cattaneo-Vernotte (CV) or Jeffreys type (dual-phase-lag) models, are necessary has been a matter of discussion. Fourier's equation only predicts diffusion phenomenon whereas non-Fourier

models predict a coupled diffusion-wave response. In this work, using classical Non-Equilibrium Molecular Dynamics (NEMD) simulations, we investigated the process of heat conduction in a three-dimensional atomic beam of finite length. Specifically, we studied solid argon modeled using a Lennard-Jones (6-12) potential and silicon modeled using a Stillinger-Weber and Tersoff potential. Langevin and Nosé Hoover thermostats were used to maintain a temperature gradient so that a heat flux vector would develop within the system. Results of the simulations in the form of spatio-temporal temperature and heat flux vector profiles were obtained and a curve fitting procedure based on the Iteratively Re-weighted Least Squares (IRLS) regression method was used to estimate the parameters appearing in the dual-phase-lag model. The figure (image right) presents the comparison of the curves obtained by the continuum dual-phase-lag model and unsteady NEMD simulations. It was found that the two relaxation times appearing in the dual-phase-lag model are almost equal and, therefore, Fourier heat conduction is adequate for modeling unsteady heat conduction for insulators – at least for the cases studied here. Despite this result, the use of the dual-phase-lag model has the advantage of providing information on relaxation times which cannot be obtained from the Fourier model alone. In addition, the above procedure also yields the thermal conductivity of the material. This result was compared with and found to be in agreement with two other procedures: Green-Kubo and direct NEMD. Of these three approaches, the curve fitting procedure described above has the advantage of taking the least amount of simulation time to calculate thermal conductivity and relaxation times. This is because the procedure is based on unsteady heat conduction and only a few spatio-temporal profiles are necessary; in contrast for the other approaches the system needs to be brought to steady state which can take a very long time.

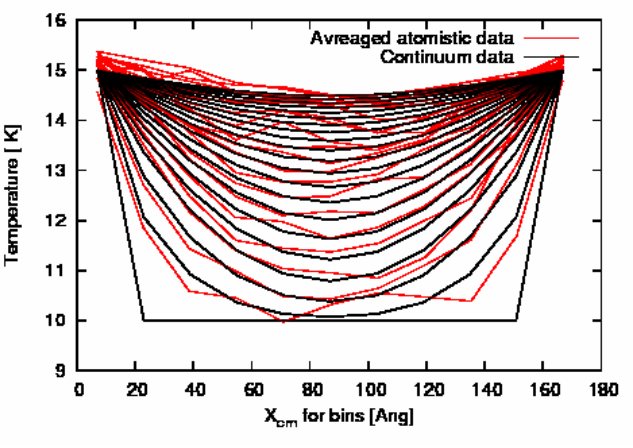

Temperature profiles obtained using NEMD simulations and a dual-phase-lag continuum model for a solid argon beam. The beam is initially equilibrated at 10 K and the temperatures of the ends are then raised and held at 15 K. The red curves are the averaged atomistic results for 6 different initial conditions and the black curves are those obtained from dual-phase-lag model using parameters obtained from the IRLS fitting procedure. The beam was divided into 11 bins and X_{cm} is the position along the beam of the center of mass of each bin in Angstroms.

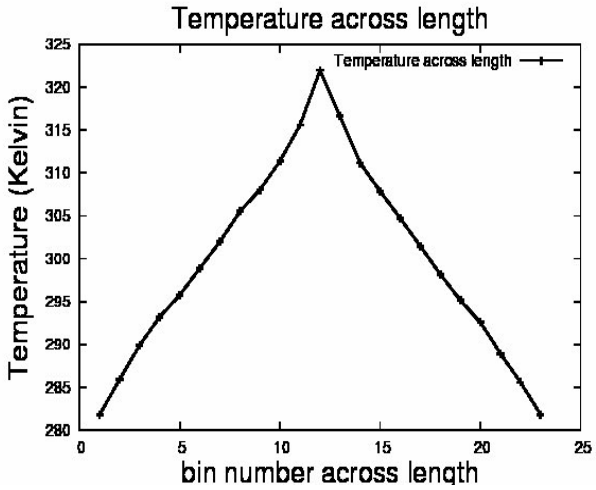

The thermal conduction in amorphous and crystalline silica material was also studied. Using the NEMD direct method and the curve-fitting procedure described above, the thermal conductivities of crystaline and amorphous silica at different temperatures have been calculated and the results are in agreement within the range of literature and experimental values. The figure (image above) shows the steady state temperture profile for the case where crystalline silica (quartz), using the BKS potential, is maintained at 280 K at the ends of the beam and 320 K tempertaure in the middle of the beam. Through the curve fitting procedures, here too, it was found that Fourier equation is sufficient to model heat transfer.

Finally, studies have been carried out to understand how heat waves travel in the atomic systems. The figure (image right) presents such a case. Here, an argon beam of size 303 x 4 x 4 is divided into 101 bins, where each bin consists of 243 atoms. Periodic boundary conditions are employed. A LJ (6-12) pair potential is used to model the atomic interactions. The middle bin of the beam is subjected to a heat pulse of 1400 femtosecond (fs) time-duration with rise and fall times of 200 fs. Initially, the temperature of the overall beam is 0K. Then, the temperature of the middle bin is increased to 20K linearly during the rise time of 200 fs. After this, its temperature is maintained at 20K for a duration of 1000 fs, which is followed by a linear downward decrease in its temperature to 0K. The rest of the beam is made to evolve under Newtonian dynamics throughout the heat pulse duration. The introduction of a heat pulse generates several waves which propagate at different speeds corresponding to different phonon modes, second sound waves, and diffusive components. The disturbances are propagating in straight lines and they are labeled as L1, L2, S1, H1, Hl, Hav, H3, corresponding to different elastic and thermal waves. Ongoing work on the hot-QC method is repeating these caculations for crystalline silica (quartz) and amorphous SiO_2.

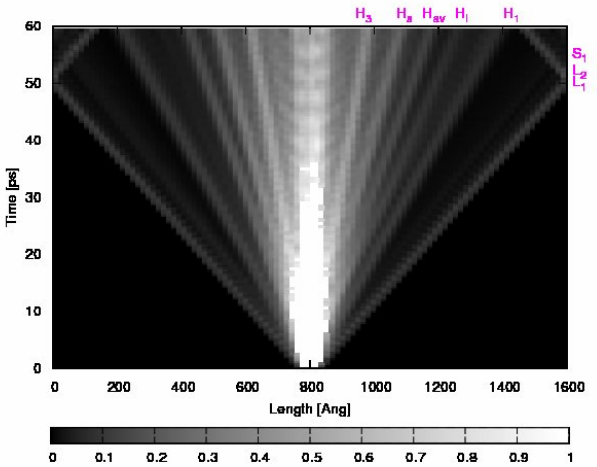

Heat wave disturbances propagating through an atomistic system.

With continued development of the hot-QC method, it should be possible to investigate the heat pulse generated by a surface reaction, in 3D through an amorphous SiO_2 surface. Specifically the transfer of energy into the bulk could be investigated, but also the influence of such heat pulses on neighboring adsorbed molecules would be of interest. Also, of interest would be correlations between the phonon characteristics of a given material and the vibrational state of desorbed (recombined) molecules. If a correlation exists, the implication would be that the accommodation coefficient (β) may depend on the material structure itself.

III.4 Development of a Finite-Rate Catalytic Model for Oxygen-Silica using Computational Chemistry

In this work we now focus on surface catalysis of atomic oxygen on silica (SiO_2). **Silica is chosen because it is a significant component in both reusable** (LI900, LI2200, FRSI) **and ablative** (SIRCA) **thermal protection systems** [24]. In addition, studies have found that several non-SiO_2 based thermal protection systems, such as SiC (at T < 1800 K) and Ultra High Temperature Ceramics (ZrB2-SiC and ZrB2-SiC-HfB2 at T < _1300 K) form thin SiO_2 layers when exposed to air plasma, and act similarly to pure silica from a catalytic perspective [22,33]. Despite a large body of experimental work there is uncertainty in the precise temperature, pressure, and gas composition dependence of heating on silica surfaces due to heterogeneous catalysis [23]. **Reported values for oxygen recombination coefficients on silica** in the literature **span several orders of magnitude** ($2x10^{-4} < \gamma < 4x10^{-1}$) at 1000 K [34-35].

The goal of this work is to develop a methodology for creating a finite rate catalytic model of oxygen recombination on silica using molecular dynamics simulations equipped with the ReaxFF potential. The ReaxFF potential is a classical potential parameterized from quantum chemical calculations, which allows for chemical reactions to occur over the course of a molecular dynamics (MD) simulation. Using MD simulations, we will identify the chemical structures on silica surfaces where recombination can occur. The elementary reactions in our finite rate catalytic model are based on the possible outcomes of oxygen interaction with these structures. Molecular dynamics simulations of individual events are used to find the parameters of the functional forms of the reactions, including activation energies and pre-exponential factors. This methodology is used to create a preliminary finite rate catalytic model, which can be used to find recombination coefficients and surface coverages at a given temperature and pressure, and can be directly incorporated into Computational Fluid Dynamics (CFD) simulations using the FRC boundary condition described in section III.1.

Realistic Amorphous SiO_2 Bulk Structures

Fundamental to any description of recombination on surface are the *in-situ* chemical structures on the surface with which gas-phase molecules interact. Our research focuses on amorphous silica (a-SiO_2) surfaces. It has been shown that Molecular Dynamics (MD) simulations with empirical potentials are able to describe the structural features on silica surfaces under standard atmospheric conditions in cases where comparison to experimental data can be made [36,37]. However, in many experiments measuring surface catalycity, surfaces are exposed to an air-plasma, and there is uncertainty if the same structures are present under these conditions. Therefore, we will use MD simulations with the ReaxFF potential to investigate the structures that occur on SiO2 surfaces before and after they are exposed to atomic oxygen. All MD simulations are run with the publicly available molecular dynamics program, LAMMPS, which is distributed by Sandia National Labs [32].

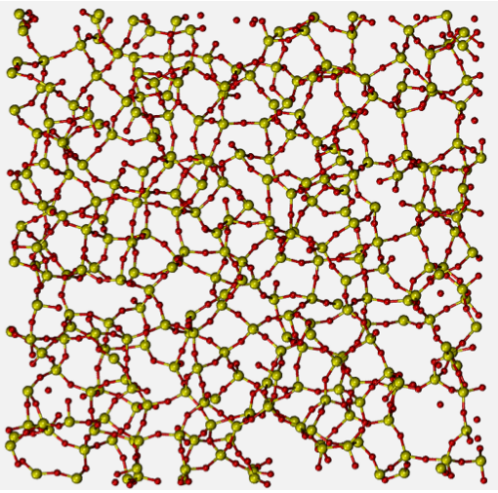

Figure 10 – Amorphous SiO2 bulk structure created by annealing β-cristobalite using ReaxFF.

Before modeling amorphous silica *surfaces*, we had to first validate that the ReaxFF potential can accurately reproduce *bulk* amorphous silica. To generate bulk a-SiO_2, we performed molecular dynamics simulations following the annealing procedure described by Hu et al.22 Bulk β-cristobalite was given an initial temperature of 8000 K, and propagated for 20 ps under NVT dynamics to randomize its initial structure. The bulk was then cooled at 50 K/ps under NVT dynamics until it reached 300 K. The system was propagated for a further 40 ps under NPT dynamics at 300 K, 1 atm, with the last 20 ps used to collect statistics about the structure. We used 11,616 atoms in our simulations, enough to ensure

sufficient statistics about the structure were collected [38]. Simulations were performed with the ReaxFF potential and the BKS potential using the modifications outlined in the work by Jee et al. [39]. An image of the resulting structure is seen in Fig. 10.

The total correlation function T(r) can be used to directly compare the computationally generated annealed bulk structure to neutron scattering experiments. This function is generated from the partial radial distribution functions as described by Nakano et al.[40] As shown in Fig. 11, the total correlation function of annealed a-SiO_2 created with both potentials is in relatively good agreement with experimental results [41]. However, the ReaxFF potential under-predicts the location and magnitude of the secondary peak, which represents the average distance between O-O nearest neighbors, as well as several tertiary peaks. The BKS potential is in better agreement with experimental measurements on bulk a-SiO_2, however, this potential lacks the ability to describe chemical reactions such as gas phase oxygen-oxygen bonding because of its two-body nature. Ref. [42] contains detailed comparisons of ReaxFF predictions to an entire set of experimental measurements including coordination numbers and angle distributions. **The ReaxFF potential was found to be in quite good agreement with experimental measurements, which lended confidence that the ReaxFF potential could adequately model bulk a-SiO_2; a pre-requisite for modeling a-SiO_2 *surfaces*.**

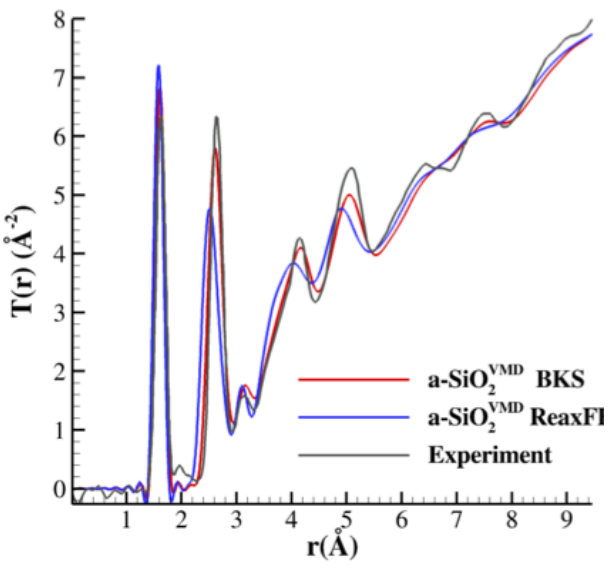

Figure 11 – Total correlation function T(r) plotted for both ReaxFF and BKS potentials compared with experiment [41].

Realistic Amorphous SiO_2 Surface Structures

The simplest way to generate an a-SiO_2 surface is to cleave the previously generated bulk along a convenient plane. However this method creates an idealized surface that is terminated by a number of highly reactive broken bonds. To generate more realistic surfaces, we performed MD annealing simulations on an a-SiO_2 surface cleaved from the previously generated bulk. To create surfaces, we followed the procedure detailed in Fogarty et al. [43] A slab of cleaved a-SiO_2 was heated at 25K/ps from 300 K to 4000 K under NVT dynamics and then cooled back to 300 K at same rate. The system was propagated for an additional 40 ps under NPT dynamics at 300 K, 1 atm with the final 20ps used to collect statistics. All slabs were 20 Angstroms thick with areas chosen so that surfaces had a statistically significant number of defects, as described in the upcoming section. In general, we found that longer annealing simulations, or additional annealing cycles, produced surfaces with slightly lower surface energies and slightly fewer defects. However, we found that the same *types* of defects occur on surfaces annealed for longer times. Therefore we are confident that although surfaces may contain more defects that they would if annealed at slower and more experimentally realistic rates, they still contain the salient structural features of an a-SiO_2 surface. We then used the annealed a-SiO_2 surfaces as a basis for realistic amorphous silica surfaces that we will subsequently expose to atomic oxygen.

Catalytic Defects on Amorphous SiO_2 Surfaces After Exposure to Dissociated Oxygen

Unlike surfaces created from crystalline bulk materials, annealed amorphous SiO_2 surfaces contain a finite number of catalytic defects (surface sites where catalytic events may be energetically favorable). However, these defects may change in number or in chemical structure when exposed to a

high temperature dissociated gas, as may be the case in air plasma experiments and hypersonic flight. In order to simulate exposure to atomic oxygen, **we used MD simulations with a novel Flux Boundary Condition (FBC); a method that exposes a surface to an ideal gas at a given temperature, pressure, and composition.** A more detailed description of this method can be found in Ref. [42]. In Flux Boundary Condition simulations, atoms are generated at random points on a plane above the surface with a frequency corresponding to the flux of an ideal gas through that plane. This plane is 10 Angstroms above the surface, beyond the force cutoff of the potential. Impinging atoms are given velocities sampled from a Maxwell-Boltzmann distribution and a random incident angle. Atoms or molecules moving away from the surface at a distance greater than 10 Angstroms are deleted, allowing us to simulate only the gas-surface interface region, and gas phase collisions in this region are rare. A diagram of this method is shown in Fig 12. Over the course of a simulation, gas atoms adsorb on the initially empty surface, which eventually reaches a steady state population of adsorbed atoms. **At steady state we can determine the concentration and nature of chemical defects for an amorphous SiO_2 surface exposed to a dissociated gas at a given temperature and pressure.**

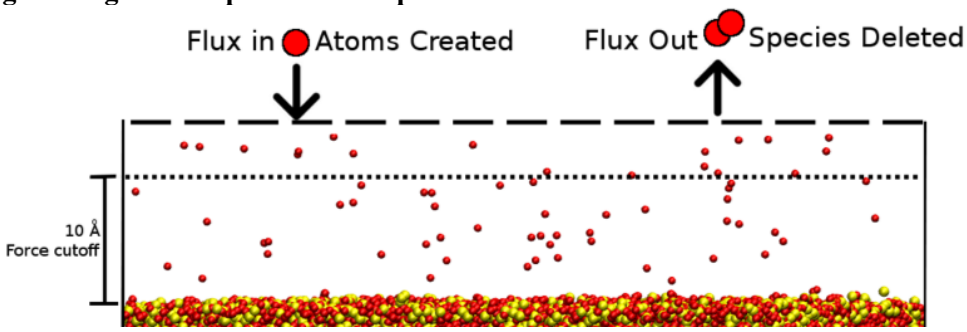

Figure 12 – Schematic of the Flux Boundary Condition simulation technique (red=oxygen, yellow=silicon)

We are primarily interested in structures on the surface where recombination can occur. The most prevalent structures are bridging oxygen atoms $(Si-O-Si)$. These bridging oxygen atoms are typical of the stable reconstructions shown much earlier in Fig. 3a, and are strongly bound to the surface (~10 eV bonding energy). The energy released in gas phase oxygen recombination is only 5.16 eV, so the direct recombination of an impinging gas-phase oxygen atom with a bridging oxygen atom is very unlikely, and thus, **these stable reconstructions are non-catalytic**. Therefore, **we expect that recombination will occur at defects on the surface.** We find that the most populous defects on surfaces exposed to atomic oxygen are the non-bridging oxygen atom $(\equiv Si-O\cdot)$ (Fig. 13b) and adsorbed molecular oxygen $(\equiv Si-O_2)$ (Fig. 13c). We also find that the annealed a-SiO_2 surfaces have a significant number of under-coordinated silicon atoms $(\equiv Si\cdot)$ (Fig. 13a) before exposure to the dissociated gas, and also during exposure when adsorbed oxygen atoms are removed due to catalytic processes.

Visualizations of SiO_2 surfaces with these defects highlighted are shown in Fig. 14. This is representative of the actual surface that gas-phase atoms interact with. Figure 14 corresponds to a high pressure, however, we have performed numerous studies showing that at lower pressures, the concentration of defects is reduced, but the defect chemistries themselves remain identical. **There is experimental evidence for the existence of the $(\equiv Si\cdot)$ and $(\equiv Si-O\cdot)$ defects on silica surfaces** under irradiation and fracture. The $(\equiv Si\cdot)$ defect has been extensively studied, and has been identified on irradiated and vacuum fractured quartz and amorphous silica using Electron Spin Resonance (ESR) [44,45]. ESR in conjunction with isotope effects have been used to identify the $(\equiv Si-O\cdot)$ defect on irradiated amorphous SiO_2. The $(\equiv Si\cdot)$ and $(\equiv Si-O\cdot)$ structures have also been observed in other MD simulations of a-SiO_2 surfaces simulated using different interatomic potentials [36,46,47]. We are not aware of any experimental evidence of the $(\equiv Si-O_2)$ structure, however recent DFT calculations performed by the Truhlar group at the University of Minnesota as part of a new AFOSR MURI project

confirm the energetics and stability of this defect. To study recombination on realistic silica surfaces, our finite rate catalytic model thus focuses on the $(\equiv Si\cdot)$, $(\equiv Si-O\cdot)$, and $(\equiv Si-O_2)$ defects (Fig. 13).

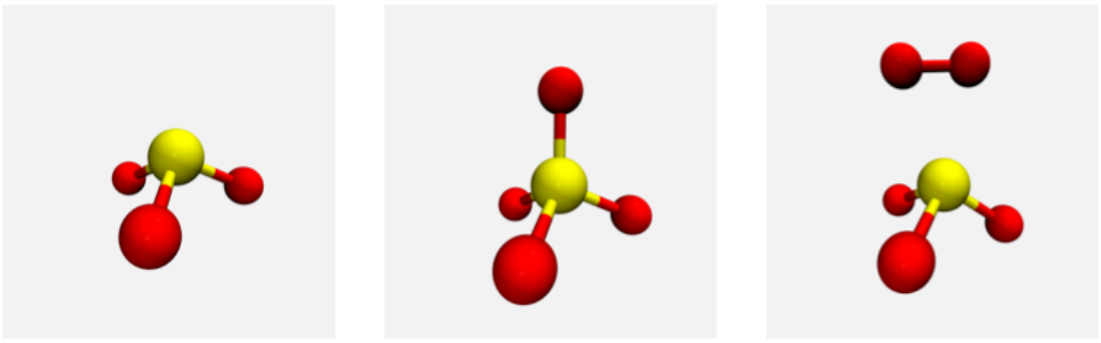

(a) $(\equiv Si\cdot)$ (b) $(\equiv Si-O\cdot)$ (c) $(\equiv Si-O_2)$

Figure 13 – Defects observed on annealed amorphous SiO2 surfaces exposed to dissociated oxygen.

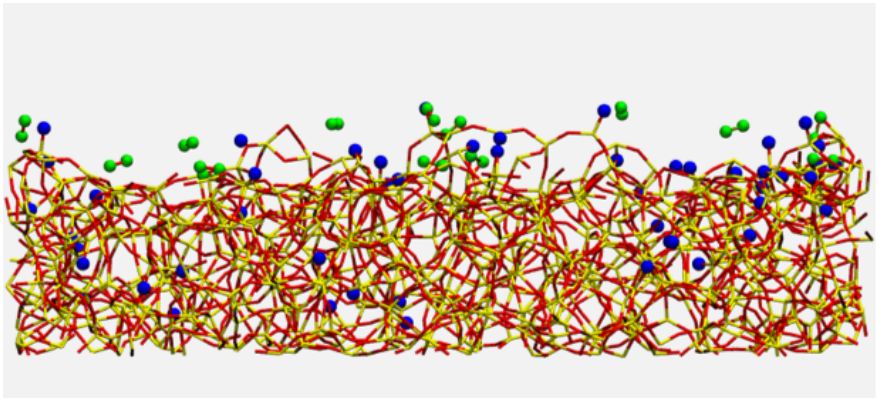

Figure 14 – Visualization of annealed amorphous SiO2 after exposure to dissociated oxygen at high pressure. Defects are highlighted. Blue = $(\equiv Si-O\cdot)$. Green = $(\equiv Si-O_2)$.

Gas-Phase Collisions with Defect Surfaces Including Off-Normal Collisions

For our finite rate catalytic model, we considered direct gas phase interactions with the $(\equiv Si\cdot)$, $(\equiv Si-O\cdot)$, and $(\equiv Si-O_2)$ defects. The rates of reactions at these defects were found with MD simulations of the collision of single gas-phase atomic oxygen atoms with the defects. Simulations were performed for isolated defects on an otherwise reconstructed surface. It can be shown that on the scale of MD simulations (Angstroms) the defect density is low and gas phase collisions occur rarely and are spread over large surface areas. Thus defects do not interact with other defects and sequential gas-phase collisions do not interact with one another. The relative energies of defect structures on the reconstructed surface are shown in Fig 15.

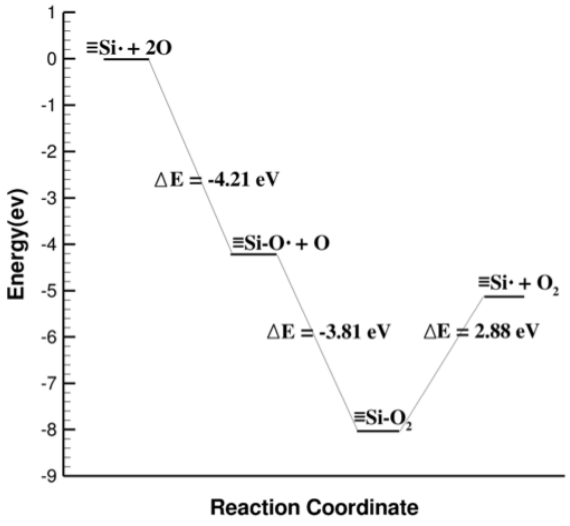

Figure 15 – Relative energy of defects.

A set of reactions was chosen based on the range of possibilities for gas phase oxygen atoms interacting with defects on the surface, as shown in Table 3. The first reaction is atomic oxygen adsorption, which is considered irreversible based on the high energy of adsorption (-4.21 eV). We have found that oxygen atoms colliding with the $(\equiv \mathrm{Si}-\mathrm{O}\cdot)$ site can either form $(\equiv \mathrm{Si}-\mathrm{O}_2)$ (reaction 2), or recombine via Eley-Rideal (ER) recombination (reaction 3). Additionally, we have observed that atomic oxygen atoms encountering $(\equiv \mathrm{Si}-\mathrm{O}_2)$ can either replace the O_2 molecule or combine with one of the oxygen atoms in the $(\equiv \mathrm{Si}-\mathrm{O}_2)$ structure via ER recombination (reaction 4). In either case the end result is identical: an absorbed atomic oxygen and a gas phase molecular oxygen. We also consider the possibility of desorption of molecular oxygen from the $(\equiv \mathrm{Si}-\mathrm{O}_2)$ site (reaction 5). The variables used in the finite rate catalytic model to describe the concentrations of defects and surface coverages are shown in Table 4. The total number of active sites [S] is constant and is equal to the sum of the concentrations of individual defects.

Mechanism	Name	
$O + \equiv Si\cdot \rightarrow \equiv Si\text{-}O\cdot$	Atomic Adsorption	(1)
$O + \equiv Si\text{-}O\cdot \rightarrow \equiv Si\text{-}O_2$	O_2 Formation	(2)
$O + \equiv Si\text{-}O\cdot \rightarrow O_2 + \equiv Si\cdot$	ER Recombination	(3)
$O + \equiv Si\text{-}O_2 \rightarrow O_2 + \equiv Si\text{-}O\cdot$	ER Recombination II/ O_2 Replacement	(4)
$\equiv Si\text{-}O_2 \rightarrow O_2 + \equiv Si\cdot$	O_2 Desorption	(5)

Table 3 – Elementary gas-surface interactions forming the finite-rate catalytic model

Surface Concentrations

$[O]_s$	Concentration of adsorbed oxygen ($\equiv$Si-O$\cdot$) on the surface (m^{-2})
$[O_2]_s$	Concentration of adsorbed molecular oxygen ($\equiv$Si-O_2) on the surface (m^{-2})
$[E]_s$	Concentration of vacant sites ($\equiv$Si$\cdot$) sites on the surface (m^{-2})
$[S]$	Total concentration of active sites on the surface (m^{-2})
	(by definition $[O]_s + [O_2]_s + [E]_s = [S]$)

Fractional Coverages

θ_O	$[O]_s$ / $[S]$
θ_{O_2}	$[O_2]_s$ / $[S]$
θ_E	$[E]_s$ / $[S]$
	(by definition $\theta_O + \theta_{O_2} + \theta_E = 1$)

Table 4 – Surface coverage variables completing the finite-rate catalytic model

Adsorption: $(O + \equiv Si\cdot \Rightarrow \equiv Si - O\cdot)$

The energy of adsorption of oxygen is -4.21 eV, as shown in the potential energy surface (PES) in Fig 16a. Given this deep potential well, we assume that the **sticking probability for O on this site is one**.

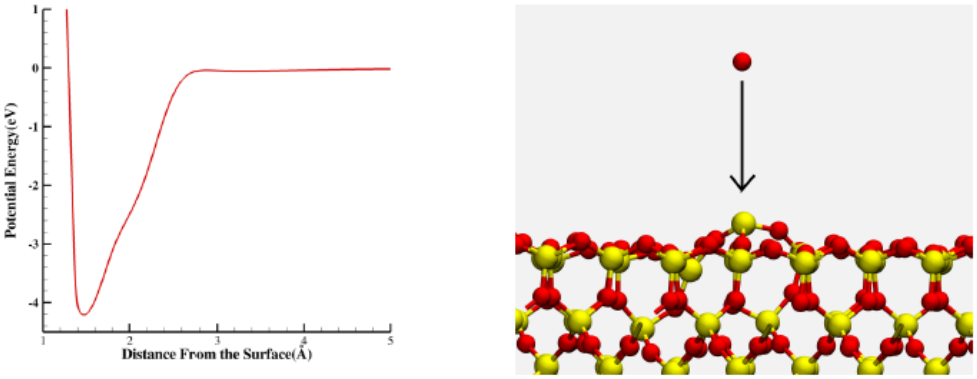

(a) PES for atomic oxygen adsorption on ≡Si·

(b) Diagram of atomic oxygen adsorption on ≡Si·

Figure 16 – Atomic oxygen adsorption on $(\equiv Si\cdot)$

Molecular Oxygen Formation and ER-Recombination:
$(O + \equiv Si - O\cdot \Rightarrow \equiv Si - O_2)$ *and* $(O + \equiv Si - O\cdot \Rightarrow O_2 + \equiv Si\cdot)$

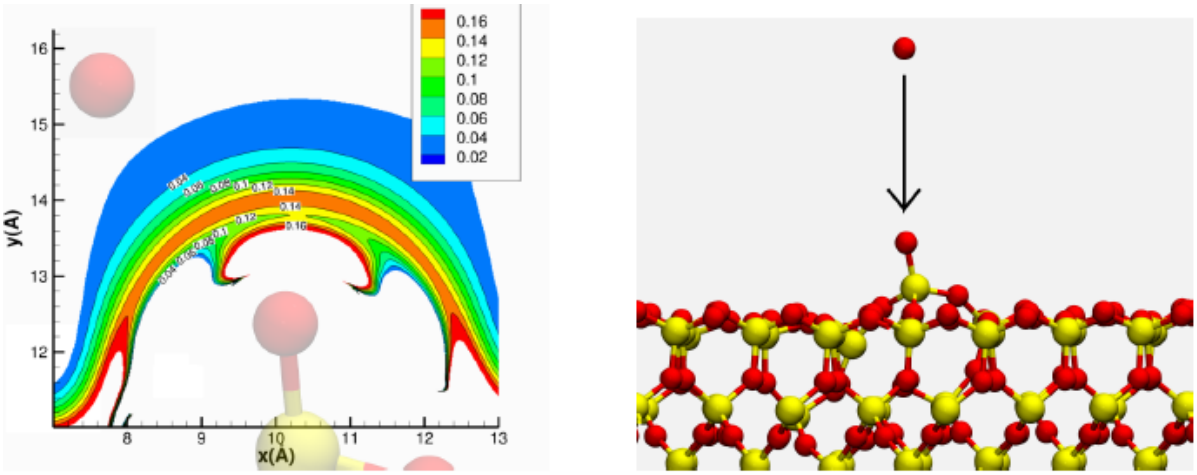

(a) PES for O_2 formation

(b) Diagram of O_2 formation simulations

Figure 17 – Molecular oxygen formation $(O + \equiv Si - O\cdot \Rightarrow \equiv Si - O_2)$

As shown in the PES in Fig. 17a, there is a well-defined transition state for O_2 formation. To find the pre-exponential factor and activation energy for this reaction, we performed molecular dynamics simulations. An oxygen atom was placed 10 Angstroms above the surface and given a velocity sampled from the Maxwell-Boltzmann distribution. The velocity of the atom was normal to the surface (off-normal collisions will be addressed in an upcoming section of the report). The atom was placed directly above the $(\equiv Si - O\cdot)$ defect and then given a random displacement parallel to the surface between 0 and 2.5 Angstroms to account for the radius of the site. To keep the surface from translating over the course of

MD simulations, the bottom atomic layer was frozen. The two atomic layers above the frozen layer were thermalized with the Langevin thermostat in order to maintain the temperature of the surface. The top seven atomic layers were allowed to move freely so as not to influence the gas-surface chemistry. Simulations were propagated until the atom collided and possibly reacted with the defect on surface. Over 2000 trajectories were carried out at each temperature, with temperatures ranging from 250-1750 K with an interval of 250 K. The results of these simulations are shown in Fig. 18a, where error bars are based on the Wald method with a 95% confidence interval. At all temperatures, the most probable reaction is O_2 formation. A log plot of the probability of O_2 formation, as seen in Fig. 18b, shows that the probability of this reaction follows an exponential trend, with **activation energy Ea = 0.149 eV**, in agreement with the PES in Fig. 17a. From the log plot, we also find that the **pre-exponential factor for this reaction is 0.85**.

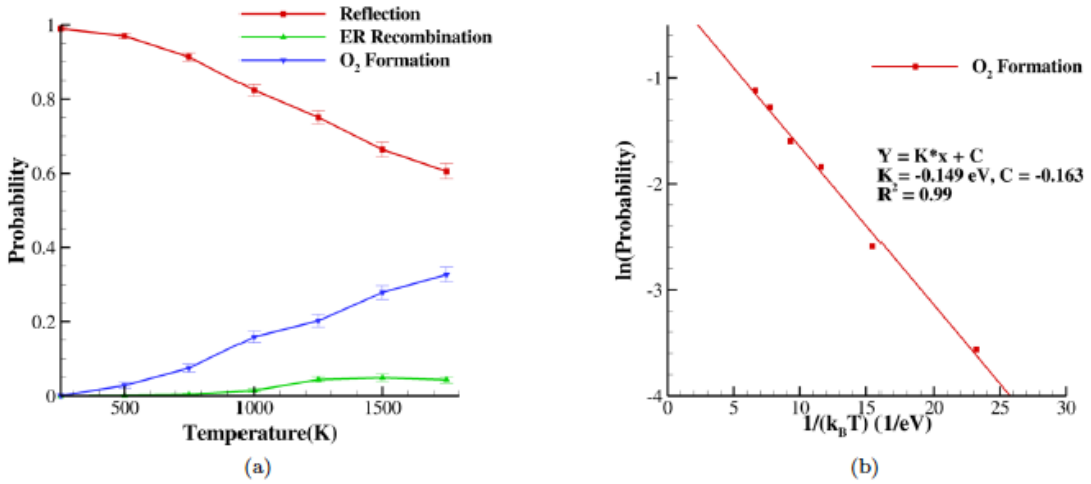

Figure 18 – Probability of O_2 formation and ER-Recombionation (a). Activation energy for O_2 formation (b).

ER-Recombination/O2 Replacement $(O + \equiv Si \cdot O_2 \Rightarrow O_2 + \equiv Si - O \cdot)$

Simulations for this reaction were carried out in an identical manner to those for O_2 formation as shown in Fig. 19. Over 4000 trajectories are carried out at each temperature. Although there are two distinct processes, for the purposes of the finite rate catalytic model we fit the sum of both processes because they produce the same result. As shown in Fig. 19b this results in an **activation energy of Ea =0.457 eV and a pre-exponential factor of 0.717**.

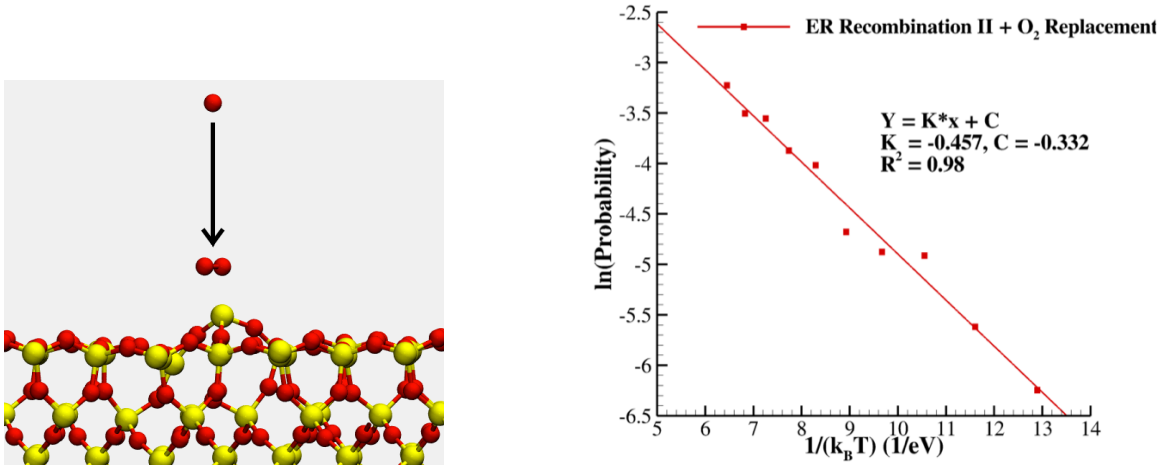

Figure 19 – O_2 Replacement simulation (a). Activation energy for O_2 Replacement + ER-Recombination (b).

Desorption of O_2 ($\equiv Si \cdot O_2 \Rightarrow O_2 + \equiv Si \cdot$)

Our results indicate that there is no significant saddle point in the PES for O_2 desorption. According to the ReaxFF potential, this PES does not significantly change for rotational conformations of the O_2 molecule in plane with the surface. Direct MD simulations of the desorption of O_2 molecules from this site would take computationally inaccessible times due to the high energy of desorption. According to transition state theory, the pre-exponential factor for the desorption of an immobile species through an immobile transition state is 10^{12} – $4x10^{13}$ [48]. Therefore we use a **pre-exponential factor of 10^{13} and an activation energy Ea= 2.88 eV** (as shown in Fig. 15) as parameters for the finite rate catalytic model.

Accounting for Off-Normal Collisions

We then analyzed the effect of off-normal collision angles on the specific reactions. In previous simulations, atoms were placed above the surface randomly within a disk with a radius of 2.5 Angstroms. For off-normal collisions, we applied a rotation matrix to the disk and the initial velocity vector of the impinging atom. This is depicted in Fig. 20 for the O_2 formation reaction.

Figure 20 shows the trajectories of many single collision simulations. In Fig. 20a, at Φ=30°, impinging atoms maintain their disk-like spatial distribution until the impact at the site, where they either react or scatter. In Fig. 20b, at Φ=75°, there is a slight distortion of the disk as it nears the surface because the surface is repulsive. By increasing the angle beyond 70°, we increase the number of atoms that enter a repulsive area above the surface before hitting the defect, decreasing the number of reacting atoms due to the fact that atoms placed in the repulsive region almost instantly scatter. In reality, atoms approaching at such angles would have encountered the repulsive region and scattered earlier in their trajectories.

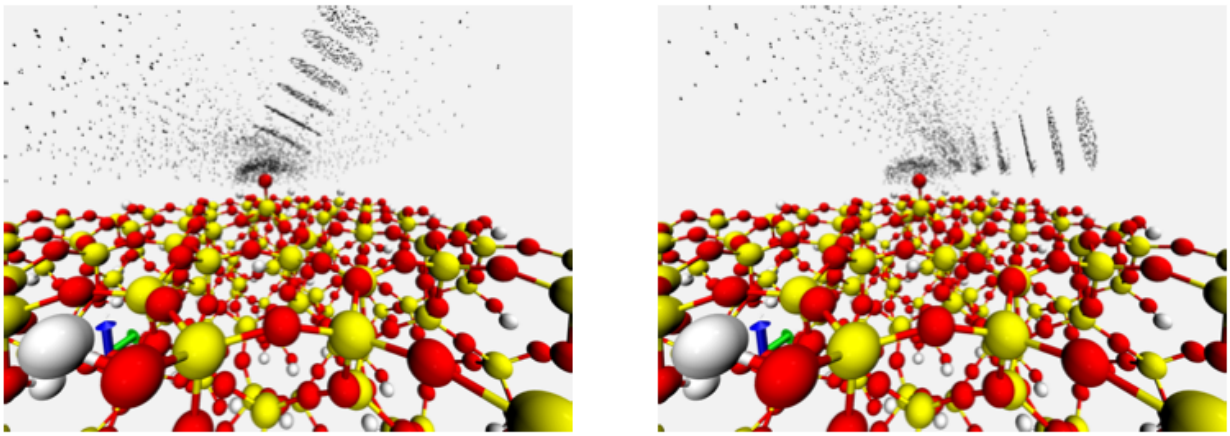

Figure 20 – Images from off-normal collision simulations of the O_2 formation reaction.

Figure 21 clearly demonstrates that the angle does affect the outcome of the O_2 formation and O_2 replacement reactions. Both these reactions are dominant mechanisms for recombination. **Thus we conclude that off-normal collisions must be accounted for when parameterizing recombination reaction rates based on molecular dynamics simulations.**

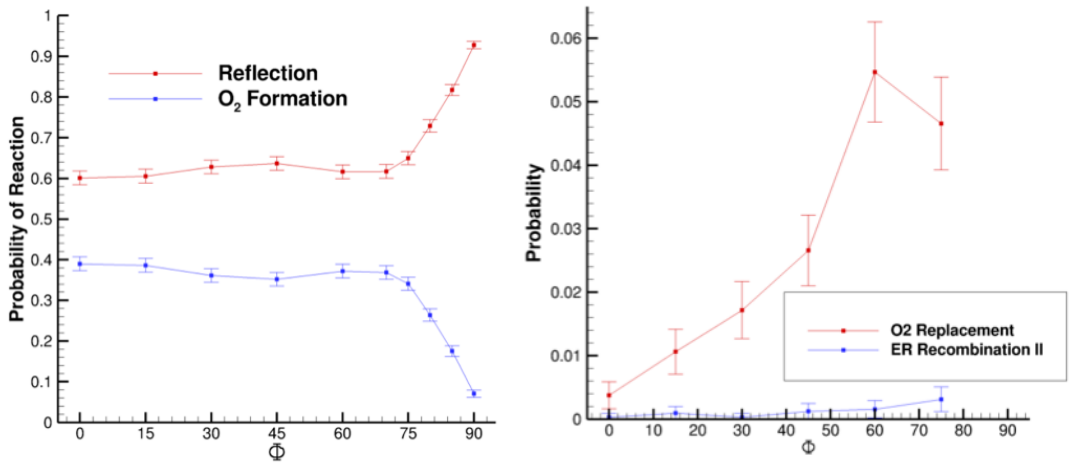

Figure 21 – Reaction probabilities in function of impact angle.

<u>The Complete Finite Rate Catalytic Model Predicted by ReaxFF</u>

The complete model, which also includes low temperature LH reactions, is completely detailed below. When used to determine recombination coefficients in function of temperature, the new FRC model can be compared with available experimental data as seen below in Fig. 22. Unlike previous researchers claims, we strongly argue that no model developed from computational chemistry is able to precisely predict the *magnitude* of experimentally inferred γ values. Since these values should scale directly with the number of active catalytic sites (the defect density) at the *macroscale*, which may be highly dependent on the material quality, surface roughness, and the gas-phase diffusion model used to interpret the experimental observations (varies for different experiments). None of these real physical considerations can be taken into account in atomistic MD simulations. However, we argue that the *trend* of γ with temperature should be predicted from computational chemistry. This trend is completely dependent on the dominant chemical reaction mechanisms, their pre-exponential factors, and activation energies; all of which are predicted by our simulations. In Fig. 22, the density of active surface sites in our FRC model was set to match the magnitude of γ found by experiment [C]. Although experimental magnitudes do not agree with each other, at high temperatures the slope of γ vs. T is somewhat consistent and our FRC model lies within the experimental uncertainty.

$O + E_c \rightleftharpoons O_c$	Atomic Oxygen Adsorption	(1)
$O + O_c \rightleftharpoons O_2 + E_c$	Eley Rideal Recombination	(2)
$O + O_c \rightleftharpoons O_{2_c}$	Molecular Oxygen Formation	(3)
$O + O_{2_c} \rightleftharpoons O_2 + O_c$	Molecular Oxygen Replacement	(4)
$O_{2_c} \rightleftharpoons O_2 + E_c$	Molecular Oxygen Desorption	(5)
$O + E_f \rightleftharpoons O_f$	Atomic Oxygen Physisorption	(6)
$O_f + E_c \rightleftharpoons E_f + O_c$	Physisorbed to Chemisorbed	(7)
$O_f + O_c \rightleftharpoons E_f + E_c + O_2$	Langmuir Hinshelwood Recombination	(8)

$[O]$	Gas Phase Atomic Oxygen Concentration	m^{-3}
$[O_2]$	Gas Phase Molecular Oxygen Concentration	m^{-3}
$[E_c]$	Empty Chemisorption Site Density	m^{-2}
$[E_f]$	Empty Physisorption Site Density	m^{-2}
$[O_c]$	Chemisorbed Atomic Oxygen Density	m^{-2}
$[O_{2_c}]$	Chemisorbed Molecular Oxygen Density	m^{-2}
$[O_f]$	Physisorbed Atomic Oxygen Density	m^{-2}
r_s	Site Radius	(m)
$\bar{c}_x$	Average speed	(m/s)

Rate	Rate Equation	Functional Form	A	E_a (eV)
r_1^f	$k_1^f[O][E_s]$	$(\bar{c}_O/4) \times (2\pi r_s^2) \times (A_1^f e^{-E_1^f/(K_B T)})$	1.0	0.0
r_1^r	$k_1^r[O_s]$	$A_1^r e^{-E_1^r/(K_B T)}$	10^{-15} (s^{-1})	4.25
r_2^f	$k_2^f[O][O_s]$	$(\bar{c}_O/4) \times (2\pi r_s^2) \times (A_2^f e^{-E_2^f/(K_B T)})$	0.169	0.401
r_2^r	$k_2^r[O_2][E_s]$	$(\bar{c}_{O_2}/4) \times (2\pi r_s^2) \times (A_2^r e^{-E_2^r/(K_B T)})$	0.663	1.27
r_3^f	$k_3^f[O][O_s]$	$(\bar{c}_O/4) \times (2\pi r_s^2) \times (A_3^f e^{-E_3^f/(K_B T)})$	1.13	0.253
r_3^r	$k_3^r[O_{2s}]$	$A_3^r e^{-E_3^r/(K_B T)}$	10^{-15} (s^{-1})	4.14
r_4^f	$k_4^f[O][O_{2s}]$	$(\bar{c}_O/4) \times (2\pi r_s^2) \times (A_4^f e^{-E_4^f/(K_B T)})$	0.172	0.303
r_4^r	$k_4^r[O_2][O_s]$	$(\bar{c}_{O_2}/4) \times (2\pi r_s^2) \times (A_4^r e^{-E_4^f/(K_B T)})$	0.716	1.18
r_5^f	$k_5^f[O_{2s}]$	$A_5^f e^{-E_5^f/(K_B T)}$	1.20×10^{14} (s^{-1})	2.71
r_5^r	$k_5^r[O_2][E_s]$	$(\bar{c}_{O_2}/4) \times (2\pi r_s^2) \times (A_5^r e^{-E_5^r/(K_B T)})$	1.0	0.0
r_6^f	$k_6^f[O][E_f]$	$(\bar{c}_O/4) \times (2\pi r_s^2) \times (A_6^f e^{-E_6^f/(K_B T)})$	1.0	0.0
r_6^r	$k_6^r[E_f]$	$(A_6^r e^{-E_6^f/(K_B T)})$	10^{15} (s^{-1})	0.130
r_7^f	$k_7^f[O][O_f][E_c]$	$(2\pi r_s \Lambda_D) \times (\bar{c}_O/4) \times P_{rc} \times (A_7^f e^{-E_7^f/(K_B T)})$	1.0	0.0
r_8^f	$k_8^f[O][O_f][O_c]$	$(2\pi r_s \Lambda_D) \times (\bar{c}_O/4) \times P_{rc} \times (A_8^f e^{-E_8^f/(K_B T)})$	1.0	0.2

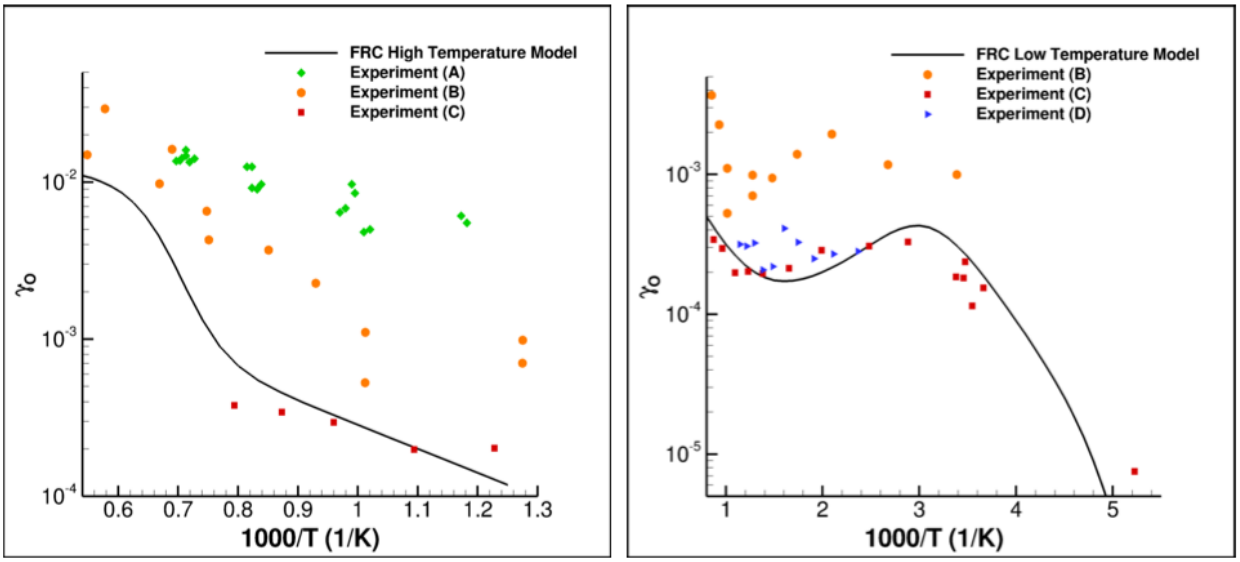

(a) High Temperature FRC Model (b) Low Temperature FRC Model

Figure 22 – Comparison of the recombination coefficients predicted by the FRC model compared to experiment. Experimental data is taken directly from the published articles listed below.

[A] Balat-Pichelin, M., Badie, J., Berjoan, R., and Boubert, P., "Recombination coefficient of atomic oxygen on ceramic materials under earth re-entry conditions by optical emission spectroscopy," Chemical Physics, Vol. 291, No. 2, 2003, pp. 181–194.

[B] Stewart, D. A., "Surface Catalysis and Characterization of Proposed Candidate TPS for Access-to-Space Vehicles," NASA Technical Memorandum 112206, 1997.

[C] Kim, Y. C. and Boudart, M., "Recombination of O, N, and H Atoms on Silica:Kinetics and Mechanism," Langmuir, Vol. 7, 1991.

[D] Marschall, J., "Experimental Determination of Oxygen and Nitrogen Recombination Coefficients at Elevated Temperature Using Laser-Induced Fluorescence," AIAA, Baltimore, MD, 1997.

IV. Publications Resulting from AFOSR Research Grant

III.1 Implementation of a Finite-Rate-Catalytic Boundary Condition in the US3D CFD Code

Sorensen, C., Valentini, P., and Schwartzentruber, T.E., "Uncertainty Analysis of Reaction Rates in a Finite Rate Surface Catalysis Model", *accepted, in-press,* ***Journal of Thermophysics and Heat Transfer***, 2011.

Sorensen, C., Valentini, P., and Schwartzentruber, T.E., "Uncertainty Analysis of Reaction Rates in a Finite Rate Surface Catalysis Model", AIAA Paper 2011-3643, June 2011, presented at the 42nd AIAA Thermophysics Conference, Honolulu, HI.

Valentini, P., Schwartzentruber, T.E., and Cozmuta, I., "A Mechanism-Based Finite-Rate Surface Catalysis Model for Simulating Reacting Flows", AIAA Paper 2009-3935, June 2009, presented at the 41st Thermophysics Conference, San Antonio, TX.

III.2 Computational Chemistry: Inter-atomic Potential and Validation for Oxygen-Platinum Systems

Valentini, P., Schwartzentruber, T.E., and Cozmuta, I., "ReaxFF Grand Canonical Monte Carlo simulation of adsorption and dissociation of oxygen on platinum (111)", ***Surface Science***, 605 (2011), pp. 1941-1950.

Valentini, P., Schwartzentruber, T.E., and Cozmuta, I., "Molecular dynamics simulation of O2 sticking on Pt(111) using the *ab initio* based ReaxFF reactive force field", ***Journal of Chemical Physics***, 133 (2010) 084703.

Valentini, P., Schwartzentruber, T.E., and Cozmuta, I., "ReaxFF atomic-level simulation of catalytic processes on platinum", AIAA Paper 2011-3645, June 2011, presented at the 42nd AIAA Thermophysics Conference, Honolulu, HI.

Valentini, P., Schwartzentruber, T.E., and Cozmuta, I., "Simulation of Gas-Surface Interactions using ReaxFF Reactive Molecular Dynamics: Oxygen Adsorption on Platinum", AIAA Paper 2010-4319, June 2010, presented at the 10th AIAA/ASME Joint Thermophysics and Heat Transfer Conference, Chicago, IL.

III.3 Quasi-Continuum Method: Heat Transfer from Surfaces into the Bulk Material

N. C. Admal and E. B. Tadmor, "Stress and Heat Flux for Arbitrary Multi-Body Potentials: A Unified Framework", ***J. Chem. Phys.,*** 134, 184106 (2011).

A. Singh and E. B. Tadmor, "Nonstationary Heat Conduction in Atomistic Systems", to be submitted to Phys. Rev. B (2012).

III.4 Computational Chemistry: A New Finite-Rate Catalytic Model for Oxygen-Silica

Norman, Schwartzentruber, T.E., and Cozmuta, I., "A Computational Chemistry Methodology for Developing an Oxygen-Silica Finite Rate Catalytic Model for Hypersonic Flows", AIAA Paper 2011-3644, June 2011, presented at the 42nd AIAA Thermophysics Conference, Honolulu, HI.

Schwartzentruber, T.E., Valentini, P., Norman, P., and Sorensen, C., "A Finite-Rate-Catalytic Model for Hypersonic Flows Informed by Molecular Dynamics", The Proceedings of the 7th Aerothermodynamics Symposium, ESA Special Publications SP-692, Brugge, Belgium, May 2011.

Norman, P., Schwartzentruber, T.E., and Cozmuta, I., "Modeling Air-SiO2 Surface Catalysis under Hypersonic Conditions with ReaxFF Molecular Dynamics", AIAA Paper 2010-4320, June 2010, presented at the 10th AIAA/ASME Joint Thermophysics and Heat Transfer Conference, Chicago, IL.

Schwartzentruber, T.E., Valentini, P., and Norman, P., "Molecular Dynamics Modeling of Hypersonic Gas-Phase and Gas-Surface Reactions", proceedings of the 27th International Symposium on Rarefied Gas Dynamics, July 2010, Monterey, CA.

V. REFERENCES:

[1] Barbato, M., Reggiani, S., Bruno, C., and Muylaert, J., "Model for Heterogeneous Catalysis on Metal Surfaces with Applications to Hypersonic Flows," Journal of Thermophysics and Heat Transfer, Vol. 14, No. 3, 2000, pp. 412–420.

[2] Wright, M.J., Olejniczak, J., Edquist, K.T., Venkatapathy, E., and Hollis, B.R., "Status of Aerothermal Modeling for Current and Future Mars Exploration Missions", IEEAC paper #1428, Version 7, December 10, 2005.

[3] Bose, D., Wright, M. J., and Palmer, G. E., "Uncertainty Analysis of Laminar Aeroheating Predictions for Mars Entries," Journal of Thermophysics and Heat Transfer, Vol. 20, No. 4, October-December 2006, pp. 652–662.

[4] Stewart, D.A., "Surface Catalysis and Characterization of Proposed Candidate TPS for Access-to-Space Vehicles", NASA Technical Memorandum 112206, July 1997, Ames Research Center.

[5] J. Marschall and M. MacLean, "Finite-Rate Surface Chemistry Model, I: Formulation and Reaction System Examples", AIAA Paper 2011-3783, presented at the 42nd AIAA Thermophysics Conference, Honolulu, Hawaii, June 2011.

[6] Rosner, D. E. and Feng, H. H., "Energy Transfer Effects of Excited Molecule Production by Surface-catalyzed Atom Recombination," Faraday Trans.I - Phys.Chem., Vol. 70, 1974, pp. 884-907.

[7] Halpern, B. and Rosner, D. E., "Chemical energy accommodation at catalyst surfaces. Flow reactor studies of the assocation of nitrogen atoms on metals at high temperatures," J. Chem. Soc., Faraday Trans. 1, Vol. 74, 1978, pp. 1883–1912.

[8] Seward, W. A. and Jumper, E. J., "Model for Oxygen Recombination on Silicon-Dioxide Surfaces," Journal of Thermophysics and Heat Transfer, Vol. 5, No. 3, 1991, pp. 284–291.

[9] Deutschmann, O., Riedel, U., and Warnatz, J., "Modeling of Nitrogen and Oxygen Recombination on Partial Catalytic Surfaces," Journal of Heat Transfer, Vol. 117, 1995, pp. 495–501.

[10] Nasuti, F., Barbato, M., and Bruno, C., "Material-Dependent Catalytic Recombination Modeling for Hypersonic Flows," Journal of Thermophysics and Heat Transfer, Vol. 10, No. 1, 1996, pp.131-136.

[11] Armenise, I., Barbato, M., Capitelli, M., and Kustova, E.V., "State to State Catalytic Models, Kinetics and Transport in Hypersonic Boundary Layers," Journal of Thermophysics and Heat Transfer, Vol.20, No. 3, 2006, pp. 465-476.

[12] Thömel, J., Lukkien, J. J., and Chazot, O., "A Multiscale Approach for Building a Mechanism based Catalysis Model for High Enthalpy CO2 Flow," 39th AIAA Thermophysics Conference, Vol. AIAA 2007-4399, June 2007.

[13] Armenise, I., Capitelli, M., and Longo, S., "Fourier and Diffusive Heat Transfer in Hypersonic Nitrogen Flows: State-to-State Approach," Journal of Thermophysics and Heat Transfer, Vol.23, No. 4, 2009, pp. 674-683.

[14] MacLean, M., Marschall, J., and Driver, D. M., "Finite-Rate Surface Chemistry Model, II: Coupling to Viscous Navier-Stokes Code," 42nd AIAA Thermophysics Conference, Honolulu, HI, Vol. AIAA Paper 2011-3784, June 2011.

[15] Bedra, L., Rutigliano, M., Pichelin, M. B., and Cacciatore, M., "Atomic Oxygen Recombination of Quartz at High Temperature: Experiments and Molecular Dynamics Simulation," Langmuir, Vol. 22, 2006, pp. 7208-7216.

[16] Cacciatore, M. and Rutigliano, M., "Eley-Rideal and Langmuir-Hinshelwood Recombination Coefficients for Oxygen on Silica Surfaces," Journal of Thermophysics and Heat Transfer, Vol. 13, No. 2, 1999.

[17] Arasa, C., Busnengo, H. F., Salin, A. and Sayos, R. [2008], 'Classical dynamics study of atomic oxygen sticking on the β-cristobalite (100) surface', Surface Science 602, 975–985.

[18] Arasa, C., Gamallo, P. and Sayos, R. [2005], 'Adsorption of atomic oxygen and nitrogen at β-

cristobalite(100): A density functional theory study', Journal of Physical Chemistry B. 109, 14954–14964.

[19] Arasa, C., Moron, V., Busnengo, H. F. and Sayos, R. [2009], 'Eley-rideal reaction dynamics between o atoms on β-cristobalite(100) surface: A new interpolated potential energy surface and classical trajectory study', Surface Science 603, 2742–2751.

[20] Moron, V., Arasa, C. and Busnengo, H. F. [2008], 'Theoretical study of O2 dissociation and reflection on the β-cristobalite(100) surface', Proceedings of the Rarefied Gas Dynamics: 26th International Symposium, AIP Conf. Proc. 1084, 682.

[21] Moron, V., Gamallo, P., Martin-Gondre, L., Crespos, C., Larregaray, P. and Sayos, R. [2011], 'Recombination and chemical energy accommodation coefficients from chemical dynamics simulations: O/O2 mixtures reaction over a β-cristobalite (001) surface', Physical Chemistry Chemical Physics pp. 17494–17504.

[22] Balat-Pichelin, M., Badie, J., Berjoan, R. and Boubert, P. [2003], 'Recombination coefficient of atomic oxygen on ceramic materials under earth re-entry conditions by optical emission spectroscopy', Chemical Physics 291(2), 181–194.

[23] Bedra, L. and Balat-Pichelin, M. J. H., "Comparative modeling study and experimental results of atomic oxygen recombination on silica-based surfaces at high temperature," Aerospace Science and Technology, Vol. 9, 2005, pp. 318-328.

[24] Cozmuta, I., "Molecular mechanisms of gas surface interactions in hypersonic flow," 39th AIAA Thermophysics Conference, Miami, FL, 2007, AIAA-2007-4046.

[25] Nompelis, I., Drayna, T. W., and Candler, G. V., "A Parallel Unstructured Implicit Solver for Reacting Flow Simulation," 17th AIAA Computational Fluid Dynamics Conference, Vol. AIAA 2005-4867, June 2005.

[26] Sorensen, C., Valentini, P., and Schwartzentruber, T. E., "Uncertainty Analysis of Reaction Rates ina Finite Rate Surface Catalysis Model," 42nd AIAA Thermophysics Conference, Honolulu, HI, Vol. AIAA Paper 2011-3643, June 2011.

[27] Van Duin, A., Dasgupta, S., Lorant, F., and Goddard, W.A. III, "ReaxFF: A Reactive Force Field for Hydrocarbons", J. of Phys. Chem. A, 2001, I05, pp. 9396-9409.

[28] Van Duin, A., Strachan, A., Stewman, S., Zhang, Q., Xu, X., and Goddard, W.A. III, "$ReaxFF_{SiO}$ Reactive Force Field for Silicon and Silicon Oxide Systems", J. of Phys. Chem. A, 2003, I07, pp. 3803-3811.

[29] D. Frenkel and B. Smit. Understanding Molecular Dynamics Simulation. Academic Press, 2002.

[30] M. P. Allen and D. J. Tildesley. Computer Simulation of Liquids. Ox- ford, 1987.

[31] S. J. Plimpton. Fast parallel algorithms for short-range molecular dy- namics. J. Comp. Phys., 117:1–19, 1995.

[32] http://lammps.sandia.gov/index.html.

[33] Alfano, D., Scatteia, L., Monteverde, F., Beche, E., and Balat, M., "Microstructural characterization of ZrB2-SiC based UHTC tested in the MESOX plasma facility," Journal of the European Ceramic Society, Vol. 30, 2010, pp. 2345-2355.

[34] Kim, Y. C. and Boudart, M., "Recombination of O, N, and H Atoms on Silica:Kinetics and Mechanism," Langmuir, Vol. 7, 1991.

[35] Carleton, K. and Marinelli, W., "Spacecraft thermal energy accommodation from atomic recombination," Journal of Thermophysics Heat Transfer, Vol. 6, 1992, pp. 650-655.

[36] Levine, S. M. and Garofalini, S. H., "A structural analysis of the vitreous silica surface via a molecular dynamics computer simulation," The Journal of Chemical Physics, Vol. 86, No. 5, 1987, pp. 2997-3002.

[37] Chen, Y., Cao, C., and Cheng, H., "Finding stable alpha-quartz surface structures via simulations," Applied Physics Letters, Vol. 93, 2008, pp. 181911.

[38] Hu_, M., Demiralp, E., Cagin, T., and Goddard, W., “Factors a_ecting molecular dynamics simulated vitreos silica structures," Journal of Non-Crystalline solids, , No. 253, 1999, pp. 133-142.

[39] Jee, S., McGaughey, A., and Sholl, D., “Molecular simulations of hydrogen and methane permeation through pore mouth modified zeolite membranes," Molecular Simulation, Vol. 35, No. 1, 2010.

[40] Nakano, A., Kalia, R., and Vashishta, P., “First sharp diffraction peak and intermediate-range order in amorphous silica: finite-size defects in molecular dynamics simulations," Journal of Non-Crystalline Solids, Vol. 171, 1994, pp. 157-163.

[41] Susman, S., Voline, K., Montague, D., and Price, D., “Temperature dependence of the first sharp diffraction peak in vitreous silica," Physical Review B., Vol. 43, No. 13, 1991.

[42] Norman, Schwartzentruber, T.E., and Cozmuta, I., “A Computational Chemistry Methodology for Developing an Oxygen-Silica Finite Rate Catalytic Model for Hypersonic Flows”, AIAA Paper 2011-3644, June 2011, presented at the 42nd AIAA Thermophysics Conference, Honolulu, HI.

[43] Fogarty, J., Aktulga, H., Grama, A., and van Duin, A., “A reactive molecular dynamics simulation of the silica water interface," The Journal of Chemical Physics, Vol. 132, 2010, pp. 174704.

[44] Warren, W., Poindexter, E., O_enberg, M., and Muller-Warmuth, W., “Paramagnetic Point Defects in Amorphous Silicon Dioxide and Amorphous Silicon Nitride thin Films," Joural of the Electrochemical Society, Vol. 139, No. 3, 1992.

[45] Costa, D., Fubini, B., Giamello, E., and Volante, M., “A novel type of active site at the surface of crystalline SiO2 (α-quartz) and its possible impact of pathogenicity," Canadian Journal of Chemistry, Vol. 69, 1991, pp. 1427-1434.

[46] Wilson, M. and Walsh, T., “Hydrolysis of the amorphous silica surface. I. Structure and dynamics of the dry surface." The Journal of Chemical Physics, Vol. 113, No. 20, 2000, pp. 9180-9190.

[47] Roder, A., Kob, W., and Binder, K., “Structure and dynamics of amorphous silica surfaces," Journal of Chemical Physics, Vol. 114, No. 17, 2001, pp. 7602-7614.

[48] Thomas, W. and Thomas, W., Principles and Practice of Heterogeneous Catalysis, VCH Publishers Inc., New York, NY. USA, 1997.